UNIVERSIDADE D
COIMBRA

Sara Inês Furtado Canário

Orchestrating Osteoclast Differentiation Through ROS and Mitochondrial Regulation: Developing new approaches for osteoporosis treatment

Dissertação no âmbito do Mestrado em Bioquímica orientada pela Doutora Vilma Marisa Arrojado Soares Sardão Oliveira e pelo Professor Doutor António Joaquim Matos Moreno e apresentada ao Departamento de Ciências da Vida da Faculdade de Ciências e Tecnologia da Universidade de Coimbra.

Janeiro de 2020

Orchestrating Osteoclast Differentiation Through ROS and Mitochondrial Regulation: Developing new approaches for osteoporosis treatment

Sara Inês Furtado Canário

Vilma Marisa Arrojado Soares Sardão Oliveira
António Joaquim Matos Moreno

Coimbra
January 2020

This work was performed at MitoXT- Mitochondrial Toxicology and Experimental Therapeutics laboratory at the Center of Neuroscience and Cell Biology of University of Coimbra, Portugal, under the supervision of Dr. Vilma Sardão (Center of Neuroscience and Cell Biology, University of Coimbra).

Institutional supervision was provided by Dr. António J. Moreno (Department of Life Sciences, University of Coimbra).

The present study was financed by European Regional Development Fund (ERDF) through the Operational Programme Competitiveness Factors-COMPETE and by FCT- Fundação Para a Ciência e Tecnologia, under research grant IF/01182/2015, POCI-01-0145-FEDER-007440.

Agradecimentos

Agradeço à Fundação Para a Ciência e Tecnologia por ter suportado financeiramente o trabalho realizado e apresentado nesta dissertação.

Ao finalizar esta etapa que começou, de certa maneira, muito antes do Mestrado em Bioquímica, não posso deixar de agradecer a todos os que contribuíram, direta ou indiretamente, para a realização do trabalho apresentado na presente dissertação.

Primeiro, à minha orientadora, Dr.ª Vilma Sardão, por me ter aceitado como sua aluna e pela maneira como me orientou e me ensinou ao longo deste período. Mas acima de tudo, quero agradecer pela paciência, calma e apoio que demonstrou em todos os momentos: quando correu bem, quando correu mal, quando os resultados não foram bem os esperados, e principalmente quando eu duvidei que conseguia.

Em segundo lugar, ao Dr. Paulo Oliveira, por me ter aceitado no seu grupo e por toda a ajuda e orientação que sempre disponibilizou.

Agradeço também ao meu coorientador, Professor Dr. António J. Moreno, por ter aceitado supervisionar o meu trabalho.

Agradeço a todos os membros do grupo MitoXT pela integração e apoio. O espírito de equipa e entreajuda que existe no laboratório, para além do bom humor constante marcaram a minha estadia, alegrando mesmo os dias menos bons. Em especial, à Adriana, quero dar o mais profundo agradecimento por todo o tempo que "perdeu" comigo, pela paciência e ajuda constante, por tudo o que me ensinou, e acima de tudo pela amizade, pelas gargalhadas partilhadas e pelo cheesecake de maracujá! À "crazy cat lady" Sara Valente, minha homónima, colega de equipa e amiga, quero agradecer também toda a ajuda e cooperação. As Saras foram uma equipa constante++ no laboratório que gosto de pensar que não vai ser esquecida facilmente. À Rafaela, à Margarida e à Gabriela, quero

agradecer todo o apoio, todos os momentos de descontração e de brincadeira e definitivamente agradecer por estarem, como eu, sempre dispostas a comer. Agradeço também ao Rui e ao Ricardo Amorim que estiveram sempre prontos a ajudar, tanto a mim como às Saras.

Quero agradecer ainda aos meus companheiros de todas as viagens Coimbra-Cantanhede/ Cantanhede-Coimbra, André e Grilo, por tornarem as viagens mais curtas com a vossa, às vezes nem tanta, boa disposição.

À minha madrinha, Ana Rita, que passou de conhecida a amiga numa agradável surpresa, muito obrigada por toda a ajuda e carinho.

À minha afilhada, Andreia, agradeço o dia no bar das matemáticas em que me pediu para ser madrinha. Desde esse dia enche-me de orgulho. Levo-a para sempre no coração.

Aos amigos que fiz em Coimbra e que levo para a vida: Tamara, Sofia, Ana Luísa, Guímaro, Ivo e Chewbacca. Muito obrigada por todos os momentos e por toda a amizade.

Às minhas eternas colegas de casa, Helena, Bia e Leoa, obrigada por terem feito parte da aventura que foi "A Congregação das Irmãs Franciscanas". Não podia ter pedido melhores pessoas para partilhar o meu mau feitio. Longe de casa, fizeram com que me sentisse em casa. Obrigada por tudo!

Às amigas de Figueiró, as de sempre e para sempre: Alexandra, Clara, Carolina, Diana, Filipa, Patrícia e Vânia. São as melhores. Obrigada pelo apoio incondicional, sempre! Por todos os cafés que eu não pude ir beber e todos os planos que falhei por estar a trabalhar na tese. Obrigada pela compreensão, carinho e amizade.

À minha família louca e única o meu muito obrigada por me terem apoiado sempre, acreditando, por vezes, mais em mim do que eu mesma. Muito obrigada por me incentivarem a ser quem sou e a querer ser ainda mais. Em especial, o maior obrigada à minha mãe e melhor amiga, sem

a qual nunca teria sido possível chegar aqui. Agradeço do fundo do coração a luta constante para que eu tivesse todas as oportunidades que nunca lhe foram dadas. Muito, muito obrigada!

Resta-me agradecer à minha pessoa, o Óscar, que não só fez parte do meu percurso académico como faz parte da minha vida. Obrigada pelo amor e pela amizade, por ser o meu porto de abrigo. Obrigada pela paciência sem fim, obrigada por me conhecer tão bem que sabe sempre o que eu preciso, mesmo que eu não saiba. Agradeço também aos meus pais emprestados Nucha e Óscar que se tornaram um apoio constante e muito importante na minha vida. Obrigada por todo o carinho.

A todos, MUITO OBRIGADA!

TABLE OF CONTENTS

RESUMO

A remodelação óssea é um processo altamente regulado e dinâmico que envolve absorção de osso antigo pelos osteoclastos e formação de nova matriz óssea pelos osteoblastos. Com o envelhecimento, há uma multitude de mudanças que ocorrem no organismo alterando a sua função e metabolismo, e a remodelação óssea não é exceção. A osteoporose é uma doença que aparece como consequência de um aumento na absorção óssea que não pode ser superado pela formação de novo osso. Este desequilíbrio resulta numa diminuição da densidade óssea e um risco aumentado de fraturas no osso que são causa de grande incapacidade por parte da população afetada. Uma vez que o estrogénio é reconhecido como um regulador importante da remodelação óssea, mulheres após menopausa são um grupo particularmente suscetível ao aparecimento de osteoporose, uma vez que há uma diminuição nos níveis desta hormona. como consequência de uma diminuição na função dos ovários. As mitocôndrias, enquanto "powerhouse" da célula, são responsáveis por múltiplos papéis no organismo, sendo muito importantes para a diferenciação celular, uma vez que alteram o seu metabolismo como resposta às necessidades energéticas da célula. O objetivo principal deste estudo foi avaliar a performance mitocondrial dos macrófagos RAW 264.7 durante a diferenciação em osteoclastos mediada por RANKL na presença e ausência de E2. Para tal, diferenciámos macrófagos RAW 264.7 em osteoclastos após exposição a 50 ng/mL de RANKL, e avaliámos como é que o RANKL interfere com a sua performance mitocondrial e produção de ROS, tanto na presença como na ausência de estradiol. Os nossos resultados demonstraram que, após 6 dias de exposição a RANKL, as células obtidas expressavam cathepsin K e TRAP, marcadores específicos de osteoclastos maduros e ativos. Adicionalmente, ao terceiro dia de exposição a RANKL, já existia um aumento dos níveis de proteína cathepsin K, mostrando que o processo de diferenciação pode começar mais cedo do que foi sugerido inicialmente pela literatura existente. No entanto, a exposição a RANKL a longo-termo (desde 1 a 6 dias) diminuiu, nas células RAW 264.7, a taxa de consumo de oxigénio (OCR) e a taxa de acidificação extracelular (ECAR), dois parâmetros usados para avaliar o metabolismo celular,

mostrando um perfil metabólico mais quiescente. Contudo, como esperado, foi observado um aumento na produção de Espécies Reativas de Oxigénio (ROS) celulares e mitocondriais, nas células RAW 264.7, após 6 dias de exposição a RANKL. O efeito agudo do RANKL no OCR e ECAR também foi avaliado. Aqui, os resultados obtidos demonstraram um aumento no OCR imediatamente após a adição de RANKL, mas nenhuma outra alteração, nem relativamente ao OCR nem ao ECAR, foram observadas após o tratamento agudo. Relativamente ao efeito do 17-β Estradiol, até ao momento, os resultados obtidos não nos permitem tirar uma conclusão firme e é necessária a realização de mais experiencias neste contexto. Contudo, os nossos resultados permitem-nos concluir que a exposição a RANKL a longo termo leva a uma diminuição no OCR e ECAR das células RAW 264.7, o que sugere uma diminuição do metabolismo celular durante a diferenciação em osteoclastos mediada por RANKL. Adicionalmente, a mitocôndria parece ter um papel relevante no processo e pode apresentar potencial enquanto alvo para o desenvolvimento de novas estratégias terapêuticas para a osteoporose.

Palavras-chave: Osteoporose; Osteoclastos; RANKL; Mitocôndria; Estradiol

ABSTRACT

Bone remodeling is a highly regulated and dynamic involving old bone resorption by osteoclasts and new bone matrix formation by osteoblasts. With aging, there are a multitude of changes that occur in the organism altering its functioning and metabolism, and bone turnover is not an exception. Osteoporosis is a disease that appears as a consequence of an increased bone resorption that cannot be overcome by bone formation. This unbalance results in a decreased bone density and increased risk of fractures that cause great disability in the affected population. Since estrogen is known to be an important regulator of bone turnover, postmenopausal women are particularly susceptible to osteoporosis appearance due to the decreased levels of this hormone, as a consequence of a declined ovarian function. Mitochondria, the cellular powerhouses, are responsible for a multitude of roles, being very important in cellular differentiation, shifting their metabolism to answer the cell energy requirements. The main goal of this study was to evaluate the mitochondrial performance RAW 264.7 macrophages during RANKL-mediated osteoclast differentiation in the presence and absence of E2. To achieve this goal, we differentiated RAW 264.7 macrophages into osteoclasts after exposure to 50 ng/mL of RANKL, and then evaluated how RANKL, both in the presence and absence of estradiol, interfered with mitochondrial performance and ROS production. Our results demonstrated that after 6 days of RANKL exposure, the obtained cells expressed cathepsin K and TRAP, hallmarks of active and mature osteoclasts. In addition, at day 3 of RANKL exposure, cathepsin K levels were already increased, showing that the differentiation process may begin earlier than it was first suggested by the literature. However, long term exposure to RANKL (for 1 to 6 days) decreased, in RAW 264.7 cells, the oxygen consumption rate (OCR) and the extracellular acidification rate (ECAR), two parameters used to assess the cellular energy metabolism, showing a more quiescent metabolic profile. However, as expected, an increase in cellular and mitochondrial Reactive Oxygen Species (ROS) was observed in RAW 264.7 cells after 6 days of exposure to RANKL. The acute effect of RANKL on OCR and ECAR of RAW 264.7 cells was also

assessed. Obtained results demonstrated an increase in OCR immediately after addition of RANKL, but no other alteration in OCR and ECAR were observed after the acute treatment. Regarding the effect of 17-β Estradiol, at the moment, the obtained results do not allow to draw a solid conclusion and more experiments are needed in this context. However, our results allow us to conclude that long term exposure to RANKL leads to a decrease in OCR and ECAR in RAW 264.7 cells, which suggest a decrease in cellular energy metabolism during RAKL-induced osteoclast differentiation. Mitochondria appear to have a relevant role in the process, and may be potential targets for the development of new therapeutic strategies for osteoporosis.

Keywords: Osteoporosis; Osteoclasts; RANKL; Mitochondria; Estradiol

Part of the present work was presented as a poster in the following conference:

Sara Canário, Adriana Carvalho, Sara Valente, Vilma Sardão. Role of estrogen on metabolic remodeling during osteoclast differentiation. 53rd Annual Scientific Meeting of the European Society for Clinical Investigation Coimbra, Portugal 22 - 24 May 2019. Abstract published in special issue of the European Journal of Clinical Investigation, Vol. 49, page 182.

LIST OF FIGURES

LIST OF TABLES

LIST OF ABBREVIATIONS

AMPK - AMP-activated protein kinase

APS – Ammonium Persulfate Solution

ATP – Adenosine Triphosphate

BMD – Bone Mass Density

BMM – Bone Marrow Macrophages

BMPs – Bone Morphogenic Proteins

BPs – Biphosphonates

BSA – Bovine Serum Albumin

c-fms – Colony-stimulating factor 1 receptor

CoA - Coenzyme A

DMEM – Dulbeco's Modified Eagle's Medium

DMSO – Dimethyl Sulfoxide

DNA – Deoxyribonucleic Acid

DTT- Dithiothreitol

E2 - 17β-Estradiol

ECAR – Extracellular Acidification Rate

ERα – Estrogen Receptor α

ERβ – Estrogen Receptor β

$FADH_2$ – Reduced Flavin Adenine Dinucleotide

FBS – Fetal Bovine Serum

FCCP – Carbonyl cyanide 4-(trifluoromethoxy) phenylhydrozone

FoxO – Forkhead Box O

GPR30 – G-coupled receptor 30

GTP – Guanosine Triphosphate

HEPES – 4- (2-hydroxyethyl)-1-piperazineethanesulfanic acid

HRP – Horseradish peroxidase

HRT – Hormone Replacement Therapy

IMM – Mitochondrial Inner Membrane

MAPK – Mitogen-activated protein kinase

M-CSF- Macrophage colony stimulating factor

mER – Membrane Estrogen Receptors

mERα – Membrane Estrogen Receptor α

mERβ – Membrane Estrogen Receptor β

MPP – 1,3-bis (4-hydroxyphenyl)-4-methyl-5-[4-(2-piperidinylethoxy) phenol]- 1Hpyrazole dihydrochloride

MSC – Mesenchymal Stem Cells

mtDNA – Mitochondrial DNA

NAD^+ - Oxidized Nicotinamide Adenine Dinucleotide

NADH – Reduced Nicotinamide Adenine Dinucleotide

nDNA – Nuclear DNA

nER – Nuclear Estrogen Receptors

NFATc1 – Nuclear factor of activated T-cells

NF-kB – Nuclear factor-kappa B

NTC – No template control

OCR – Oxygen Consumption Rate

OPG – Osteoprotegerin

OSCAR - Osteoclast-associated immunoglobulin-like receptor

OxPHOS – Oxidative Phosphorylation

PBS – Phosphate-buffered saline

PCR – Polymerase Chain Reaction

PHTPP - 4-[2-phenyl-5,7-bis (trifluoromethyl) pyrazole [1,5-a]-pyrimidin-3-yl] phenol

PVDF – Polyvinylidene difluoride

qRT-PCR – Quantitative real time polymerase chain reaction

RANK – Receptor activator of nuclear factor kappa B

RANKL – Receptor activator of nuclear factor kappa B ligand

RNA – Ribonucleic Acid

ROS – Reactive Oxygen Species

Runx2 – Runt-related transcription factor 2

SD – Standard Deviation

SDS – Sodium Dodecyl Sulphate

SDS-PAGE – SDS-polyacrylamide gels

SEM – Standard Error of the Mean

SERM – Selective Estrogen Receptor Modulators

Sirt1 – Sirtuin 1

Sirt3 – Sirtuin 3

SOD – Superoxide Dismutase

SOD2 – Superoxide Dismutase 2

SRB – Sulforhodamine B

TBS-T – Tris-buffered saline supplemented with 0,1% Tween 20

TCA – Tricarboxylic Acid

TCA – Trichloroacetic acid (in Materials and Methods only)

TEMED - Tetramethylethylenediamine

TRAF – Tumor necrosis factor receptor-association factor

TRAP – Tartrate Resistant Acid Phosphatase

WHO – World Health Organization

1. INTRODUCTION

1.1. The Bone Tissue

The adult human skeleton is composed of a total of 206 bones which are articulated by ligaments, cartilage, and tendons that promote the connection between muscle and bone allowing the skeleton movement. Bones can be classified into long bones, short bones, irregular bones or flat bones accordingly to their form and size. Long bones are divided in epiphysis, diaphysis, and metaphysis which correspond to the bone end, shaft and the shaft end, respectively. These different parts, on their turn, possess different bone densities. The epiphysis is constituted by cortical bone which is a compact type of bone found on the external bone surface. Diaphysis and metaphysis are constituted by cancellous bone, or trabecular bone, which is more spongy and porous[1].

The skeleton plays a vital role in many body functions such as structural support of soft tissues, locomotion, and movement, protection of the internal organs, sustenance of mineral homeostasis and it also provides conditions for occurrence of the hematopoietic process in the bone narrow[2]. The connective tissue that constitutes the bone is in constant remodeling process and it contains four main types of functionally and morphologically different cells: osteoblasts, bone lining cells, osteoclasts, and osteocytes. Each cell type plays a different role in bone remodeling which is a tightly regulated process that consists of old bone reabsorption and new bone formation[3,4].

1.1.1. The Bone Remodeling Process

The osteoblasts are cuboidal cells that comprise 4 to 6 % of total bone cells. In the human body, they have origin in mesenchymal stem cells (MSC) through a process called osteoblastogenesis, where autocrine and paracrine factors such as Wnt pathway, bone morphogenetic proteins (BMPs), circulating hormones and sex steroids regulate their differentiation and activity[5,6]. Osteoblasts are

called bone forming-cells as they are responsible for synthesizing new organic matrix, specifically they secrete mainly collagen type I proteins, osteocalcin, osteopontin, osteonectin, fibronectin, bone sialoprotein II and growth factors[3].

Along the bone formation process, some osteoblast differentiate to become fully functional osteocytes becoming surrounded by bone matrix. Osteocytes, on their turn, comprise about 90 to 95% of the total amount of bone cells and are responsible for regulating both osteoblasts and osteoclasts activity being an important factor in a balanced bone remodeling[7]. This happens because osteocytes are the main cell type to produce the cytokine receptor activator of nuclear factor kappa B ligand (RANKL)[8]. This ligand is crucial for osteoclastogenesis meaning that its production is determinant to regulate bone remodeling, especially the reabsorption process, which is provided by osteoclasts[9]. Additionally, RANKL is also produced by osteoblasts, bone lining cells, and other cell types in response to different stimulation[8,10]. Bone lining cells, on the other hand, are osteoblasts that suffer an alternative differentiation and become quiescent. These cells function in a way to achieve the required osteoblast density to bone formation and also have a very important role in promoting osteoclastogenesis since they also express RANKL[11,12].

Osteoclasts are multinucleated cells that differentiate from hematopoietic lineage[13] (**Fig. 1A**). Osteoclastogenesis involves the fusion of the mononuclear precursor cells, in a process regulated by two major cytokines: the macrophage colony-stimulating factor (M-CSF) and the previously mentioned RANKL (**Fig. 1B**).

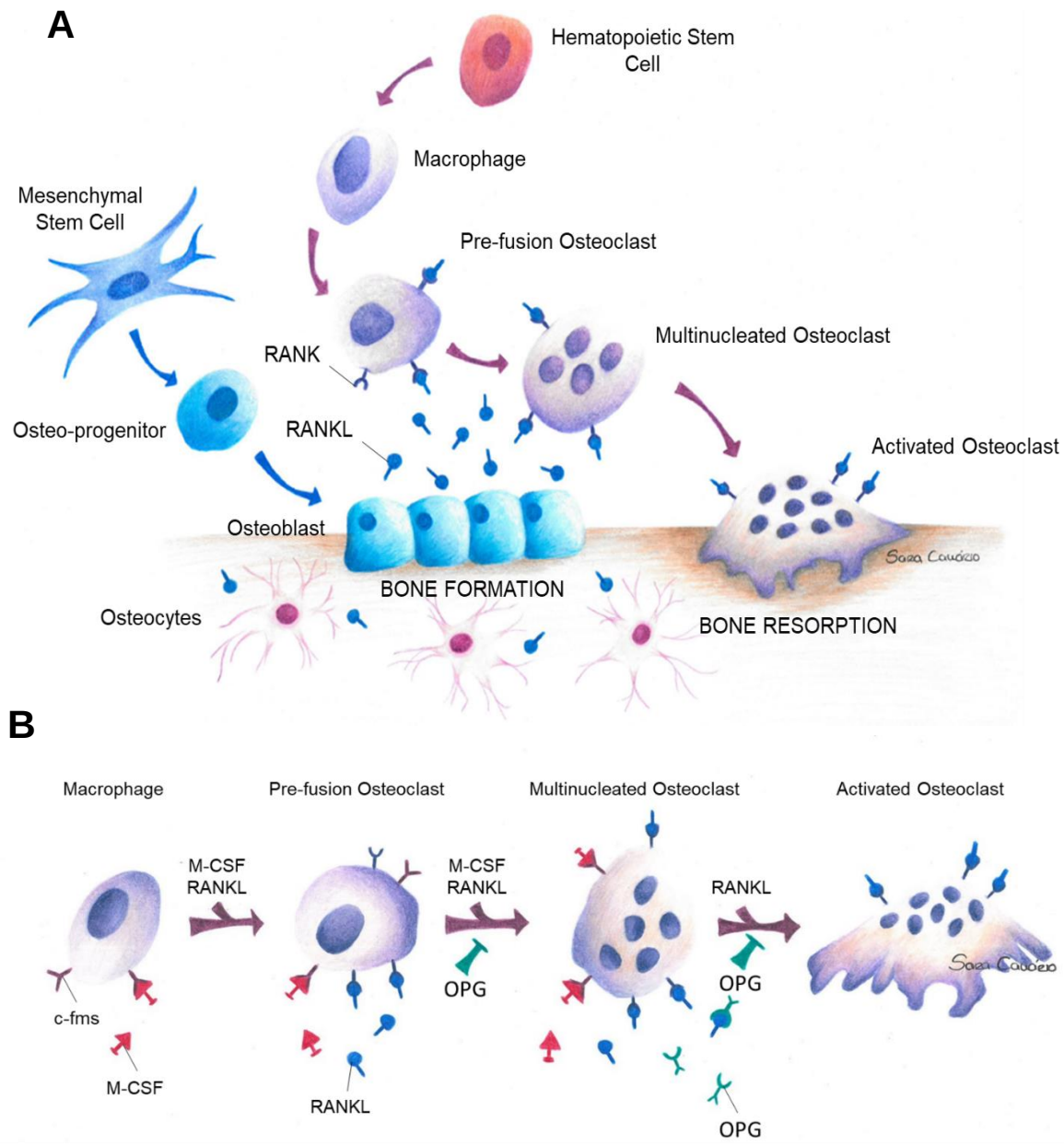

Figure 1. A) Osteoclasts and osteoblasts origin and differentiation. Osteoblasts are originated from mesenchymal stem cells and are responsible for bone formation, while osteoclasts are originated from hematopoietic stem cells and are responsible for old bone resorption. Osteoblasts and osteocytes produce RANKL which binds to receptor activator of nuclear factor kappa B (RANK) in osteoclasts precursors surface promoting osteoclastogenesis. **B)** M-CSF binding to colony-stimulating factor 1 receptor (c-fms) on macrophages surface promote cellular fusion contributing for RANKL-mediated osteoclast differentiation. Osteoprotegerin (OPG) negatively control osteoclastogenesis by binding RANKL and, therefore, preventing its bonding to RANK.

Here M- CSF links to its receptor c-fms on the osteoclast precursors surface and increases cell survival while RANKL is the actual responsible for differentiation into mature osteoclasts[14]. RANKL binding to its receptors (RANK) expressed on both osteoclast precursor and osteoclasts will trigger osteoclast differentiation by recruiting tumor necrosis factor receptor-associated factor (TRAF) 6. TRAF 6 on its turn will trigger a variety of signaling cascades that will lead to the activation of pathways such as nuclear factor-kappa B (NF-kB), mitogen-activated protein kinase (MAPK), c-fos and nuclear factor of activated T cells (NFATc1), resulting in the activation of osteoclastic genes and consequently mature osteoclasts generation (**Fig. 2**)[15-16].

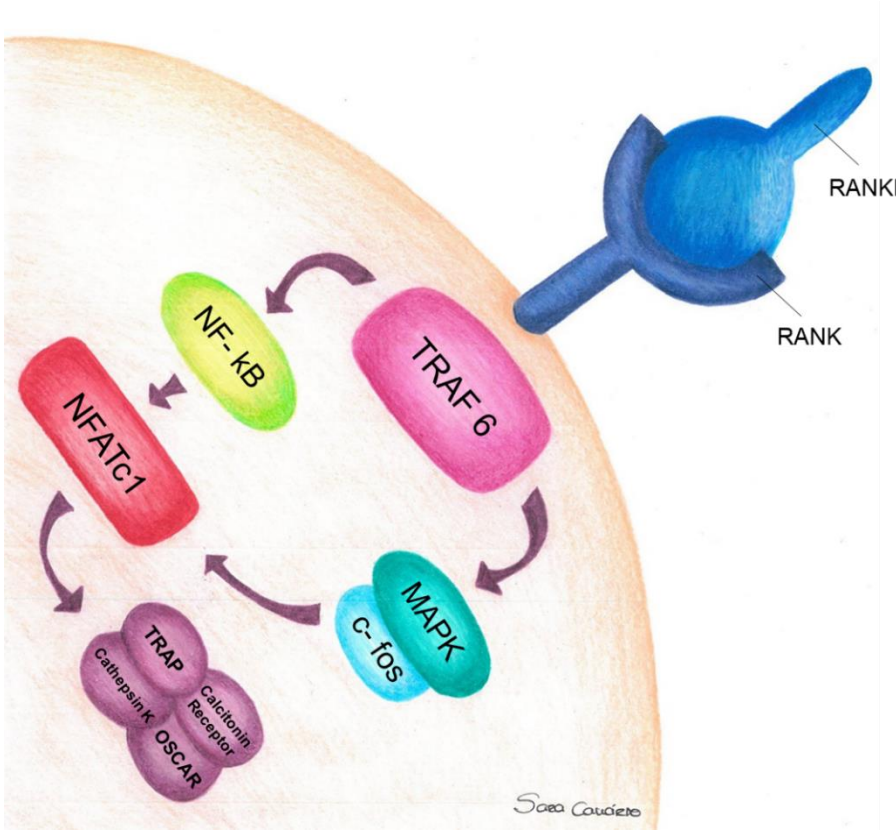

Figure 2. Signaling cascade promoted by RANKL binding to RANK. RANKL binding to its receptor on osteoclast precursor's surface leads to TRAF 6 recruitment which promotes the activation of NF-kB and MAPK pathways. MAPK activation, on its turn, leads to c-fos activation, which together with NF-kB, promotes NFATc1 activation. Ultimately, NFATc1 promotes the activation of osteoclastic genes such as Tartrate Resistant Acid Phosphatase (TRAP), Osteoclast-associated immunoglobulin-like receptor (OSCAR), Cathepsin K and Calcitonin Receptor.

Another important regulator of osteoclast differentiation is osteoprotegerin (OPG). This hormone is produced by osteoblasts and its main function is to prevent osteoclast differentiation. Osteoprotegerin binds RANKL and prevents its interaction with RANK playing an important role in maintaining the balance between osteoblasts and osteoclasts cell number and between bone formation and bone resorption (**Fig. 1B**)[17].

1.2. Osteoporosis

When bone homeostasis is affected as a result of unbalanced bone remodeling there are a series of consequences that can result from it. One of the consequences is the appearance of osteoporosis as a result of increased bone resorption that cannot be overcome by bone formation. Osteoporosis is a disease characterized by a decrease in bone density and quality resulting in a more porous and fragile bone with increased risk of fracture[18]. There are several risk factors that are taken into account when it comes to developing osteoporosis. There are risks that are lifestyle dependent, such as poor nutrition, alcohol, smoking, insufficient exercise, while others do not depend on individual habits such as age, gender, family history of osteoporosis, ethnicity, menopause, rheumatoid arthritis, endocrine disorders and exposure to certain therapies and medication [19–22]. Warfarin, for example, is a drug prescribed to patients in order to treat blood clots and decrease the risk of thrombosis or stroke occurrence. The anticoagulant action of Warfarin results from its antagonist effect on vitamin K. Several lines of evidence had shown that warfarin continued therapy leads to a decrease in bone mineral density and increased risk of bone fracture due to vitamin K deficiency. Therefore, its continued use is highly associated with osteoporosis development[23]. Drugs prescribed for breast cancer treatment are also highly associated with bone loss. Generally, chemotherapy is associated with great and severe side effects, but breast cancer therapy can be associated with the use of aromatase inhibitors, preventing estrogen production and diminishing its

regulatory effect on bone remodeling. The resultant altered bone turnover is associated with a higher risk of developing osteoporosis[24].

1.2.1. Mitochondria and Osteoporosis

1.2.1.1. Respiratory Metabolism

The cellular aerobic respiration can be divided into three main processes: oxidation of macromolecules, mitochondrial tricarboxylic acid (TCA) cycle, and mitochondrial electron transport. These processes are essential for energy production and to provide important intermediates for other cellular metabolic pathways[25].

Glycolysis occurs in the cell cytosol and consists of the oxidation of glucose into pyruvate. This is an oxygen-independent pathway with a net output of 2 molecules of Adenosine Triphosphate (ATP), 2 molecules of Reduced Nicotinamide Adenine Dinucleotide (NADH) and 2 molecules of pyruvate[26]. After glycolysis, in aerobic conditions, the pyruvate molecules are transported to the mitochondrial matrix where they can be converted to acetyl-coA by pyruvate dehydrogenase, and enter the TCA cycle[27]. Furthermore, acetyl-coA can also be provided by the catabolism of fatty acids and amino acids[28].

The TCA cycle is the cell central route responsible for fulfilling its energy and macromolecules needs, and redox balance requirements[29]. In this metabolic cyclic pathway, the oxidation of each molecule of acetyl-coA results in the generation of 3 molecules of NADH, 1 Reduced Flavin Adenine Dinucleotide ($FADH_2$), 1 molecule of Guanosine Triphosphate (GTP) and release of 2 molecules of CO_2. The NADH molecules produced both in glycolysis and in the TCA cycle, together with succinate, an intermediate of the TCA cycle, are substrates for the electron transport chain[30].

The electron transport chain is localized in the mitochondrial inner membrane (IMM) and it is constituted by NADH Dehydrogenase-ubiquinone Oxidoreductase or Complex I, Succinate Dehydrogenase-ubiquinone Oxidoreductase or Complex II, Ubiquinone-cytochrome-c Oxidoreductase or Complex III and Cytochrome-c Oxidase or Complex IV[31]. Complex I and Complex II are responsible for accepting electrons from NADH and succinate, respectively. Complex I transfers two electrons from NADH to ubiquinone, also known as coenzyme Q_{10}, which is a molecule capable of diffusing within and across the IMM. This electron transfer is coupled with proton translocation from the mitochondrial matrix to the intermembrane space. Complex II, on its turn, transfers two electrons from succinate to ubiquinone. Ubiquinone, receiving the electrons from either complex becomes reduced (ubiquinol) and diffuses to complex III where it is oxidized again. Complex III is also responsible for cytochrome c reduction. Cytochrome c is a cardiolipin-bound protein localized in the outer leaflet of IMM responsible for the electron transfer from Complex III to mitochondrial Complex IV. In complex IV, O_2 is reduced to H_2O, requiring the transfer of four electrons from cytochrome c along with the passage of four protons from the mitochondrial matrix to the intermembrane space. The extrusion of proton along the electron transport chain creates a proton motive force that can be used by ATP synthase to produce ATP[31–33].

In anaerobic conditions the pyruvate produced by the catabolism of amino acids or glucose has a different fate than in the previously described scenario. In the absence of O_2, pyruvate is reduced to lactate by lactate dehydrogenase regenerating Oxidized Nicotinamide Adenine Dinucleotide ($NAD^{+)}$ from NADH. The lactate production and its accumulation lead to an acidic pH[34,35]. In addition, there are cells that show an increased glycolytic profile independent of the presence of oxygen, leading to lactate production. For example, in tumors, the cells shift to a glycolytic profile to rapidly obtain energy from glucose catabolism downregulating mitochondrial oxidative phosphorylation, a process called Warburg Effect[36].

1.2.1.2. Mitochondrial Reactive Oxygen Species

Reactive oxygen species (ROS) are reactive forms of molecular oxygen that occur naturally in the cell and play an important role as signaling molecules, regulating metabolic and regulatory pathways[37]. There are several types of ROS including superoxide ($O_2^{-\bullet}$), hydrogen peroxide (H_2O_2), hydroxyl radical (OH^-) and singlet oxygen ($^1O_2$) and their production can result from different cellular reactions. Peroxisomes, endoplasmic reticulum and mitochondria are examples of the main endogenous sources of ROS [38,39].

Focusing on mitochondria, ROS production can occur within the electron transport chain particularly in Complex I and Complex III. In these complexes, the occasional leak of electrons to oxygen leads to $O_2^{-\bullet}$ formation which constitutes the main ROS type existent in mitochondria[40]. Once produced, $O_2^{-\bullet}$ can be converted to H_2O_2 either spontaneously or in a reaction catalyzed by superoxide dismutase (SOD)[41]. All other mitochondrial existing ROS are derived from these two species which have shown to have a great impact on cellular signaling pathways, metabolism, and biosynthetic processes[41,42].

However, at high concentrations, ROS can become toxic to the cell causing several types of damage including lipid peroxidation, carbonylation of proteins or mitochondrial DNA (mtDNA) oxidative damage. These actions constitute a condition referred to as oxidative stress. In this sense, mitochondria developed tightly controlled antioxidant defense systems that work synergistically to intercept ROS and minimize the oxidative damage. The balance between antioxidant defenses and ROS production within mitochondria, and in the cell in general, is crucial to maintain cellular homeostasis and function[43,44].

1.2.1.3. Aging Associated Metabolism and Osteoporosis

Along the aging process, there are a large number of alterations that occur in the human body metabolism which can lead to altered bone turnover, an incisive cause of osteoporosis. In women, the decrease in estrogen levels is a consequence of a decline in ovarian function and it is a determinant cause for the development of postmenopausal osteoporosis. There is evidence that estrogen is responsible for inhibiting RANKL-induced osteoclast differentiation, being one of the major regulators of bone metabolism[45,46]. In uninjured bone, estrogen inhibits osteoblasts apoptosis but stimulates apoptosis in osteoclasts, contributing to an equilibrium in bone remodeling (**Fig. 3**)[47]. Furthermore, several studies have shown that estrogen has antioxidant properties playing a decisive role in attenuating oxidative damage in the body[48,49]. This damage aggravates with aging, when increased production of reactive oxygen species is observed, and worsen in menopausal women since a drop in estrogen levels will lead to a more significant ROS effect on the organism. These alterations will be responsible for a high loss of bone mass and consequently age-related osteoporosis[48,50].

Besides being the powerhouse of the cell mitochondria are in charge of a multitude of roles such as cellular differentiation and apoptosis, regulation of ionic balance, intermediate metabolism and ROS production[51]. In this context, several studies indicate that RANKL is a stimulator of ROS production and that ROS are determinant for RANKL-induced osteoclasts differentiation specially H_2O_2 which is also required for their survival (**Fig. 3**)[52,53]. In agreement with this, there are evidence suggesting that Forkhead Box O (FoxO) proteins, a family of transcription factors, play a role in restraining osteoclast formation by preventing H_2O_2 accumulation in osteoclasts and respective progenitors. This happens through an increase in catalase expression that promotes the cellular cycle arrest and thereby osteoclasts apoptosis. In fact, the increase in ROS production mediated by RANKL is due, in part, to inhibition of FoxO-mediated transcription of catalase[54]. In addition, previous to this study the same research group had already found out that FoxOs promote survival of mature osteoblast and attenuates their apoptosis. This suggests that FoxOs are important in the quality-control

of bone remodeling. Thus, the regulation of mitochondrial oxidative stress may be a novel therapeutic strategy for osteoporosis[55].

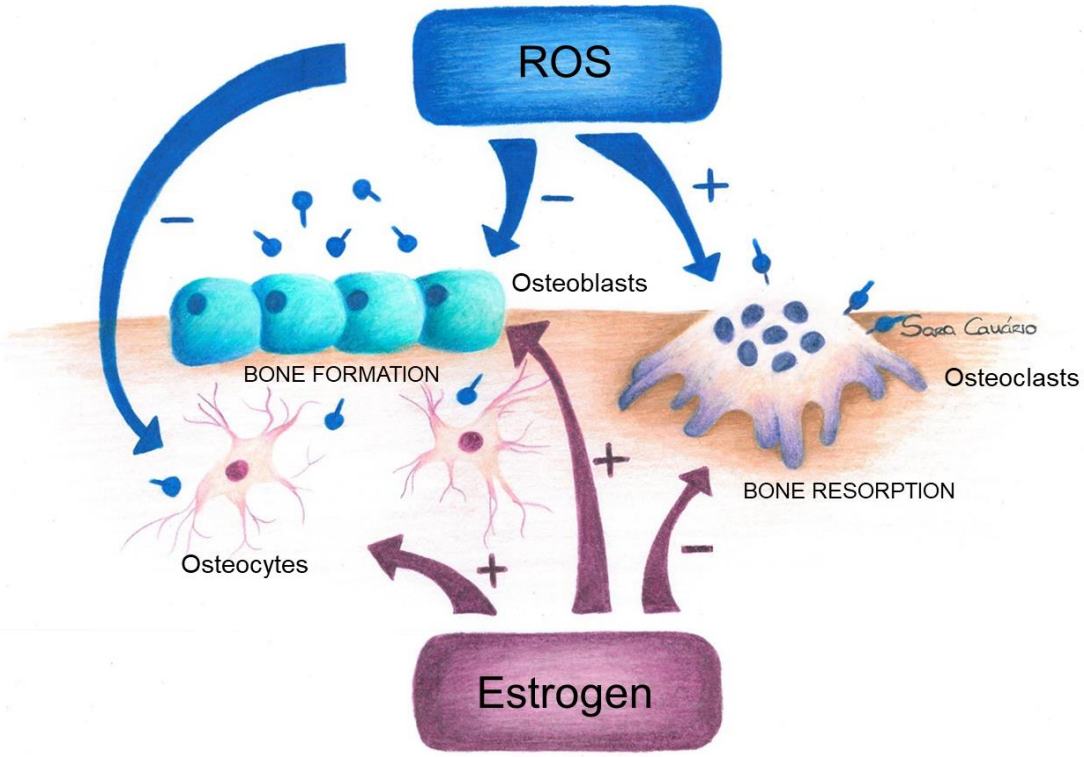

Figure 3. Effect of ROS and estrogen in bone remodeling process. ROS are determinant to promote RANKL-mediated osteoclast differentiation and therefore bone resorption, having a negative impact in bone formation. Opposing their effect is estrogen, which seems to play an antioxidant role. Estrogen improves bone resorption by promoting osteoblast differentiation and inhibits osteoclastogenesis, therefore preventing an increased bone resorption.

Also relating mitochondrial activity with osteoclast differentiation there is the mitochondrial family of Sirtuins. Sirtuins are responsible for a wide range of cellular processes, being the regulation of ROS production one of them[56]. In fact, sirtuin1 (Sirt1) has been found to suppress osteoclastogenesis by FoxOs deacetylation and thereby promote FoxO-mediated transcription and prevent ROS accumulation in osteoclasts[57]. Other recent studies have shown that sirtuin3 (Sirt3)

maintains bone homeostasis and that decreased Sirt3 levels may lead to a phenotype resembling the one that results from the aging process since it is responsible for regulating mitochondrial ROS[58]. These findings may be an important stepping point in the discovery of novel therapeutic strategies for osteoporosis based on the molecular mechanisms that control Sirtuins activity. It is also possible that Sirtuins can serve as a mediating bridge between estrogen, ROS production, and osteoclast differentiation, reinforcing the importance of mitochondria to bone remodeling[59].

1.2.2. Osteoporosis Incidence, Etiology, Risk Factors, and Diagnosis

Based on the World Health Organization (WHO) the diagnosis of osteoporosis is based on Bone Mass Density (BMD) T-scores that describe the patients in terms of standard deviations (SDs). These show how a certain group differs from the mean peak value of healthy young adults of the same sex. Thereby it is positive diagnosed osteoporosis when the BMD is equal or more than 2.5 SDs below the group mean of reference [60].

Based on WHO diagnostic criteria there are approximately 22 million women and 5.5 million men aged between 50-84 years old that are estimated to have osteoporosis only in the European Union[61]. This represents a huge osteoporotic incidence in the population than has obvious effects on the economic fraction. In 2010, in the European Union the financial burden inherent to osteoporosis was estimated to be about 37 billion euros from which costs of treatment for incident fractures represented 66% of the value, pharmacological prevention 5% and the general long-term fracture care represented 29%[61].

The common appearance of fractures is another major consequence of osteoporosis incidence. Worldwide, about 1 in 3 women over the age of 50 will experience osteoporotic fractures, as will 1 in 5 men aged over 50[62,63]. Furthermore, osteoporotic fractures lead to a great disability in the affected population. In Europe, the disability due to osteoporosis is bigger than the one caused by cancer, with

the only exception of lung cancer, and in addition, it is comparable to the disability caused by some chronic diseases, such as rheumatoid arthritis, asthma and high blood pressure related with heart disease[64].

1.2.3. Osteoporosis Associated Therapies

There have been a lot of developed therapies and drugs that aim osteoporosis treatment or improvement of its symptoms. For example, hormone-replacement therapy (HRT) was for a long time the major therapeutic option to manage post-menopausal osteoporosis. HRT consists in the administration of estrogens alone or in combination with progestin aiming a slower bone turnover and an increase in BMD decreasing risk of fracture occurence[65]. However, HRT causes severe side effects such as breast cancer, heart disease and stroke occurrence which leads to an understandable reluctance to its use[66]. Another osteoporosis therapeutic method consists in the administration of bisphosphonates (BPs) which are inhibitors of osteoclast activity and therefore of bone resorption[67]. Still, it was found that the continued administration of BPs leads to a microdamage accumulation that might compromise bone strength and delay fracture healing[68].

Furthermore, there are a lot of other options for osteoporosis management such as: antibody administration (Denosumab)[69], Selective Estrogen Receptor Modulators (SERM) such as Raloxifene[70] or Bazedoxifene[71], Calcitonin injection[72], Strontium Ranelate administration[73], Teriparatide[74] and surgical procedures such as Vertebroplasty and Kyphoplasty[75]. However, all of these strategies present significant side effects highlighting the need for new osteoporotic therapeutic strategies.

In conclusion, the great incidence of osteoporosis worldwide, its influence on the economic sector and the lack of therapies without significant side effects, are three substantial factors that highlight the importance and relevance of the present project.

1.3. Estrogen Receptors in Bone

Estrogens are a family of steroid hormones with an important physiological role regulating organism homeostasis[76]. There are three main types of estrogen, which include estradiol, estrone and estriol, being 17β-estradiol (E2) the most abundant type of estrogen in circulation[77]. In the organism, the cellular signaling of any estrogen is mediated by estrogen receptors. Estrogen receptors are a family of proteins, divided into two main groups according to their localization: Nuclear Estrogen Receptors (nER) and Membrane Estrogen Receptors (mER)[78,79].

1.3.1. Nuclear Estrogen Receptors

Estrogen Receptor Alpha (ERα) and Estrogen Receptor Beta (ERβ) are the two main groups of Nuclear Estrogen Receptors and both play a crucial role regulating bone homeostasis among their additional functions in the rest of the organism[80]. ERα and ERβ are expressed by bone cells, such osteoclasts, osteoblasts and osteocytes and their mechanism of action rely on their ability to bind DNA and modulate the expression of specific genes functioning as transcription factors[81,82]. Despite having similar structures and mechanism of action ERα and ERβ antagonize each other's actions in many tissues, including bone[83].

Previous studies performed in mice demonstrated that the deletion of ERα in osteoblast progenitors led to a reduction in cortical and trabecular bone thickness while the deletion of ERβ resulted in increased trabecular bone thickness and unchanged cortical bone[84,85]. Regarding the osteoclasts, the knockout of ERα in osteoclast precursors in mice resulted in an increased number of mature osteoclasts suggesting that ERα suppresses osteoclastogenesis and therefore bone resorption. In addition, the deletion of ERα in mature osteoclasts led to a decreased trabecular bone volume highlighting once again the importance of this receptor regulating bone resorption[86]. These conclusions are also supported by the opposite outcome that seems to be observed in osteoblasts,

where the estrogen binding to ERα enhances osteoblastogenesis promoting bone matrix formation[87]. In more detail, besides inhibiting osteoclastogenesis, ERα is also involved in regulating the life span of mature osteoclasts by expression of Fas ligand, an apoptotic factor responsive to estrogen[88].

In conclusion, all previous findings suggest that Nuclear Estrogen Receptors, namely ERα, play a major role controlling bone turnover and selective agonists for this receptor in specific may be an option as a novel therapeutic approach for osteoporosis[89,90].

1.3.2. Membrane Estrogen Receptors

Membrane Estrogen Receptors and Nuclear Estrogen Receptors have a similar weight and affinity for estrogen, however, their mechanism of action seems to be different[91]. Receptors located on the cellular membrane are on its majority G-protein-coupled receptors that induce a fast response rapidly altering cell signaling and modulating intracellular cascades[92]. Different Membrane Estrogen Receptors, involved in the regulation of bone turnover, have been identified, including the G-protein-coupled receptor 30 (GPR30), Membrane Estrogen Receptor Alpha (mERα) and Membrane Estrogen Receptor Beta (mERβ)[93,94].

Focusing on bone, besides ERα, ERβ, mERα, and mERβ, GPR30 can be expressed by osteoclasts, osteoblasts and osteocytes and it seems to play an important role maintaining homeostasis in bone turnover[95]. Previous studies have confirmed that GPR30 contributes to bone mass regulation showing that GPR30-deficient mice developed decreased bone mass and mineralization[96]. This outcome can be explained by the fact that Runt-related transcription factor 2 (Runx2), already described as an important factor for osteoblast differentiation, increases cellular proliferation in osteoblast progenitors by upregulating *Gpr30* gene expression. More specifically, estrogen regulates Runx2 expression and activity, and therefore *Gpr30* expression, which, on its turn, will activate the transcription of osteoblast-specific proteins [97,98]. Moreover, GPR30 also seems to be involved in the downregulation of osteoclast differentiation[99].

Membrane ERα and ERβ are the resultant forms of the attachment of ERα and ERβto the cellular membrane, respectively. This occurs when estrogen receptors suffer palmitoylation and bind caveolins, a family of integrative membrane proteins that act as scaffolding proteins[100]. Palmitoylation consists of the covalent attachment of fatty acids that will allow a protein-protein interaction of the receptors with caveolin-1. Once at the membrane, ERα and ERβ are able to interact with G protein alpha and beta subunits developing a fast cellular response upon estrogen binding[101]. In bone, mERα was demonstrated to be crucial promoting estrogen signaling specially in trabecular bone[102]. Specifically, in osteoblasts it was shown that the estrogen response for approximately one-third of total estrogen regulated genes is dependent on mERα signaling. No studies were performed regarding mERβ importance in bone turnover specifically, although it is thought to play a regulatory role in estrogen response alongside mERα[102,103].

1.3.3. Estrogen Receptor Antagonists

1,3-bis (4-hydroxyphenyl)-4-methyl-5-[4-(2-piperidinylethoxy) phenol]- 1Hpyrazole dihydrochloride (MPP) and 4-[2-phenyl-5,7-bis (trifluoromethyl) pyrazole [1,5-a]-pyrimidin-3-yl] phenol (PHTPP) are two synthetic highly selective antagonists for ERα and ERβ respectively. These antagonists are molecules that are able to bind estrogen receptors due to their similarity to the estrogen molecule. This leads to the receptor blockage and therefore impairment of estrogen binding and action[104]. In agreement with this, several studies where these synthetic antagonists were used have proven their inhibitory action regarding estrogen. For example, the culture of rat hippocampal neurons in the presence of both MPP and PHTPP resulted in increased neuronal death, when compared to controls, upon glucose deprivation. This outcome was a consequence of a diminished estrogen action, which is already known to have a neuroprotective effect[105]. Furthermore, another example is that the administration of these antagonists in mice promotes a blockage in actin polymerization. MPP and

PHTPP combined mediate E2 role regulating actin cytoskeleton reorganization since ERα and ERβ play an important role in this process[106].

Although no studies were performed in bone using MPP and PHTPP, there are several lines of evidence that prove them to be effective blockers of estrogen action through the mean of mERα and mERβ bonding. Taking this into account, we assumed that a similar result would occur in bone cells when exposed to these antagonists. Therefore both MPP and PHTPP were used in the present study as antagonists of E2 action, regulating its effect in the bone remodeling process.

2. HYPOTHESIS AND OBJECTIVE

Osteoporosis and osteoporosis-associated fractures have become an issue with increased importance for public health as a result of an expanding aging population[107]. Postmenopausal women are particularly susceptible to develop osteoporosis since in menopause there is an estrogen deficiency that results in impaired normal bone turnover[108]. The present study focuses on the cells involved in bone turnover, in specific, the osteoclasts, responsible for old bone resorption. Taking into account that mitochondria are crucial for many cellular processes, being one of them the cellular differentiation, we assumed that this organelle would be relevant in bone turnover and an important factor to take into account regarding osteoporosis development. Furthermore, mitochondria are responsible for ROS production. Since ROS seem to play an important role in RANKL-mediated osteoclast differentiation, our hypothesis is that RANKL-mediated osteoclast differentiation underlies important alterations in mitochondrial activity which vary in the presence or absence of estrogen/estrogen receptors.

The main goal of this study can be divided into two different principal objectives:

1. Differentiate RAW 264.7 macrophages into mature osteoclasts upon exposure to RANKL;

2. Evaluate alterations in mitochondrial performance during RANKL-mediated osteoclast differentiation in the presence and absence of E2.

Altogether the importance of the present work relies on the possibility to discover new targets that may allow the development of new therapeutic strategies for osteoporosis.

3. MATERIALS AND METHODS

3.1. Reagents

Table 1. List of reagents used in the present study with respective reference and brand from which they were obtained.

Reagent	Brand	Reference	Brand Headquarters
40% Acrylamide/Bis Solution	Bio-Rad	161-0148	Hercules, California, USA
Absolute Ethanol (200 proof) Molecular Biology Grade	Fisher Scientific	BP2818100	Waltham, Massachusetts, USA
Acetate Buffer	Sigma	3863	St. Louis, MO, USA
Agilent Seahorse XF Calibrant, pH=7.4	Agilent Technologies	100840-000	Santa Clara, California, USA
Ammonium Persulfate Solution (APS)	Gerbu	1708.0020	Heidelberg, Germany
Antibiotic/Antimycotic	Gibco	15240-062	Waltham, Massachusetts, USA (Fisher Scientific)
Antimycin A	Sigma	A8674	St. Louis, MO, USA
Blotting-Grade Blocker	Bio-Rad	170-6404	Hercules, California, USA
Bovine Serum Albumin (BSA)	Fisher Scientific	23209	Waltham, Massachusetts, USA
Bradford Reagent	Bio-Rad	500-0006	Hercules, California, USA
Charcoal, Dextran Coated	Sigma	C6241	St. Louis, MO, USA
Chloroform	Sigma	650498	St. Louis, MO, USA
Clarity Western ECL Substrate	Bio-Rad	170-5061	Hercules, California, USA
CM-H_2DCFDA	Fisher Scientific	C6827	Waltham, Massachusetts, USA
D-Glucose	Sigma	G7021	St. Louis, MO, USA
Dimethyl Sulfoxide (DMSO)	Fisher Scientific	D/4121/PB17	Waltham, Massachusetts, USA
Distilled Water DNase/ RNase Free	Gibco	10977-035	Waltham, Massachusetts, USA (Fisher Scientific)
Dithiothreitol (DTT)	Sigma	D9163	St. Louis, MO, USA
Dulbecco's Modified Eagle's Medium (DMEM)	Sigma	D5030	St. Louis, MO, USA
Estradiol	Sigma	E1024	St. Louis, MO, USA
Ethanol	PanReac AppliChem	121086.1212	Barcelona, Spain
Fast Garnet GBC Salt	Sigma	F8761	St. Louis, MO, USA
FCCP	Santa Cruz	sc203578	Dallas, Texas, USA

Fetal Bovine Serum (FBS)	Gibco	10270-106	Waltham, Massachusetts, USA (Fisher Scientific)
Glacial Acetic Acid	PanReac AppliChem	131008.1611	Barcelona, Spain
Glycerol	Sigma	G6279	St. Louis, MO, USA
Glycine	Fisher Scientific	BP381-1	Waltham, Massachusetts, USA
Guanidine Hydrochloride	Fisher Scientific	BP178	Waltham, Massachusetts, USA
HEPES	Sigma	H4034	St. Louis, MO, USA
Hoechst 33342	Fisher Scientific	H1399	Waltham, Massachusetts, USA
Hydrogen Peroxide Solution	Sigma	95294	St. Louis, MO, USA
Isopropanol	Sigma	190764	St. Louis, MO, USA
L-Glutamine	Sigma	G3126	St. Louis, MO, USA
Methanol	Sigma	M/4000/17	St. Louis, MO, USA
MitoSOX™ Red	Fisher Scientific	M36008	Waltham, Massachusetts, USA
MPP Dihydrochloride Hydrate	Sigma	M7068	St. Louis, MO, USA
Naphthol_AS_BI phosphoric acid in dimethyl formamide	Sigma	3864	St. Louis, MO, USA
Oligomycin	Sigma	O4876	St. Louis, MO, USA
Paraformaldehyde	Sigma	47608	St. Louis, MO, USA
PHTPP	Sigma	SML1355	St. Louis, MO, USA
Ponceau S	Sigma	P3504	St. Louis, MO, USA
Potassium Dihydrogen Orthophosphate (KH_2PO_4)	Fisher Scientific	P/4806/60	Waltham, Massachusetts, USA
Precision Plus Protein™ WesternC™ Standards	Bio-Rad	161-0376	Hercules, California, USA
Precision Protein™ StrepTactin-HRP Conjugate	Bio-Rad	161-0381	Hercules, California, USA
PureZOL™ RNA Isolation Reagent	Bio-Rad	732-6890	Hercules, California, USA
Receptor activator of nuclear factor kappa-B ligand (RANKL)	Sigma	R0525	St. Louis, MO, USA
Rotenone	Sigma	R8875	St. Louis, MO, USA
Sodium Bicarbonate	Sigma	S6014	St. Louis, MO, USA
Sodium Chloride (NaCl)	Sigma	71376	St. Louis, MO, USA
Sodium Dodecyl Sulphate (SDS)	Bio-Rad	161-0301	Hercules, California, USA
Sodium Phosphate Dibasic (Na_2HPO_4)	Labkem	SOPH-02A-500	Dublin, Ireland
Sodium Phosphate Monobasic (NaH_2PO_4)	Labkem	SODH-01A-500	Dublin, Ireland
Sodium Pyruvate	Sigma	P2256	St. Louis, MO, USA
SsoFast™ EvaGreen® Supermix	Bio-Rad	172-5204	Hercules, California, USA

Sulforhodamine B	Sigma	S9012	St. Louis, MO, USA
Tartrate Solution	Sigma	3873	St. Louis, MO, USA
Tetramethylethylenediamine (TEMED)	Nzytech	MB03501	Lisbon, Portugal
Trans-Blot® TurboTM 5x Transfer Buffer	Bio-Rad	10026938	Hercules, California, USA
Trichloroacetic acid (TCA)	Sigma	T0699	St. Louis, MO, USA
Tris – HCl, 0.5M pH=6.8	Bio-Rad	161-0799	Hercules, California, USA
Tris – HCl, 1.5M pH=8.8	Bio-Rad	161-0798	Hercules, California, USA
Tris Base	Fisher Scientific	BP152-1	Waltham, Massachusetts, USA
Tween® 20	Sigma	P9416	St. Louis, MO, USA

3.2. Cell Line and Culture Conditions

The biological model used in the present study was the *Mus musculus* RAW 264.7 macrophage cell line purchased from ATCC (Manassas, VA; catalog #TIB-71). Accordingly with the manufacturer's instructions, the cells were stored at liquid nitrogen vapor phase in growth medium supplemented with 5% DMSO at passage #4. RAW 264.7 macrophages were cultured in T-75 flasks, in DMEM medium supplemented with 25 mM Glucose, 4 mM L-Glutamine, 1 mM Sodium Pyruvate, 18 mM Sodium Bicarbonate, 0.1 mM NaH_2PO_4, 10% FBS, and 1% Antibiotic/Antimycotic at a final pH of 7.2, at 37ºC in a humidified atmosphere of 5% CO_2. Cells were splitted at a sub-cultivation ratio of 1:6 after reaching about 90% confluence being removed with a cell scraper and subcultured in T-75 containing 14 mL of fresh culture medium. Only the cells between passages 4 and 20 were used to avoid loss of ability to differentiate into osteoclasts[109].

3.2.1. Charcoal Stripped Culture Medium

Charcoal Stripped Culture Medium was used in assays where it was important to assess the role of estrogen and estrogen receptors on osteoclast differentiation. This medium has the same composition as described before, but the FBS used was previously treated with dextran-coated charcoal. The treatment with activated dextran-coated charcoal promotes a reduction of steroids, lipids and several hormones from the serum[110]. This procedure allowed to remove estrogens from FBS that could interfere with our results.

Thus, 5 g of Charcoal, Dextran Coated, was added to 250 ml of FBS and the serum was left on a shaker table to mix gently overnight at 4ºC. After this, the charcoal was removed from the suspension by centrifugation at 2000xg for 15 minutes and the resulting top layer was carefully removed by aspiration. The resulting FBS was aliquoted and stored at -20ºC.

3.3. Differentiation Process and Osteoclast Formation

The differentiation of RAW 264.7 macrophage into osteoclasts was induced by the addition of 50 ng/mL of RANKL to the culture medium. Cells were seeded at an optimized density of 15 625 cells/cm^2 for differentiation and after 2 days the culture medium was replaced by fresh medium with 50 ng/mL of RANKL. After 3 days the differentiation medium is renewed with the same concentration of RANKL and after a total of 6 days the differentiation process was complete (**Fig. 4**). Cells that were not exposed to RANKL and therefore undifferentiated were considered the control group.

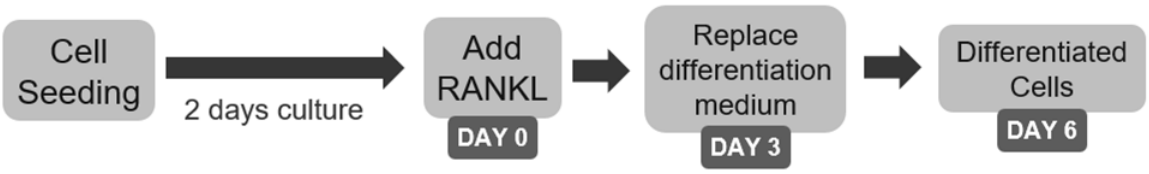

Figure 4. Experimental design of RAW 264.7 differentiation into osteoclasts.

3.4. TRAP and Hoescht Staining

Tartrate Resistant Acid Phosphatase **(**TRAP) staining, along with Hoechst staining, was performed at day 6 after RANKL addition to RAW 264.7. TRAP is an important protein present in mature osteoclasts that provides them the ability to degrade skeletal phosphoproteins and therefore it is important in bone resorption[111]. Hoechst is a cell-permeant nucleic acid dye that emits blue fluorescence when bound to double strained DNA, labeling the cellular nucleus. These two staining techniques together allow the identification of mature osteoclasts since they are defined as TRAP-positive multinucleated cells with 3 or more nuclei[112].

In this assay, cells were plated in 96 multi-well plates and differentiation was induced upon exposure to RANKL during 3 and 6 days. In the day of the assay, after aspirating the differentiation medium, cells were incubated with 1 µg/mL of Hoechst 33342 diluted in cell culture medium for 30 minutes at 37ºC in the dark. After, cells were washed with PBS and fixed with 1% paraformaldehyde diluted in phosphate-buffered saline (PBS) during 15 minutes at room temperature. Following, and in order to permeabilize the cells for the TRAP staining, cells were washed again with PBS and incubated with methanol for 30 minutes at -20ºC. This procedure was followed by another wash with milli-Q water, and after cells were incubated for 1h at 37ºC in the dark with a previously prepared TRAP staining solution.

The TRAP staining kit contains 4 reagents: Naphthol_AS_BI phosphoric acid in dimethyl formamide, 2.5 M Acetate Buffer, 0.67 M Tartrate Solution and Fast Garnet GBC Salt. In order to prepare the TRAP staining solution for a final volume of 10 mL (100 µL added per well) 0.4 mL of which one of the 3 first reagents are mixed with 8.8 mL of pre-heated milli-Q water (37ºC) followed by a quick vortex. Next 3 mg of Fast Garnet GBC salt was added followed by another quick vortex. Then the solution was filtrated through Whatman #1 paper and used immediately.

After incubation cells were washed several times with milli-Q water and 100 µL PBS was added per well to prevent cells from drying, so Hoechst's fluorescence would not be compromised. Finally, the stained cells were observed by epi-fluorescence microscopy using a Nikon Eclipse Ti-S (Nikon, Melville, NY, USA). In this experiment a total of 3 replicates per condition were formed, including control. For each replicate were taken 5 pictures of random microscope fields both for TRAP (bright field) and for Hoechst (using the UV filter). Images were obtained using the NIS Elements Imaging Software version 4.20 with a magnification of 40x. Obtained pictures were processed in ImageJ software and cells were counted manually. Cells that presented a darker color (TRAP positive) and 3 or more nuclei were considered mature osteoclasts. Cells that didn't fit the criteria were counted as not fully differentiated. The medium value between all the microscope fields of all replicates allowed to obtain the percentage of mature osteoclasts.

3.5. Protein Analysis by Western Blot

3.5.1. Protein Isolation

For protein extraction cells were seeded in 12 well plates at a density of 15 625 cells/cm^2 and three main condition groups were established: cells with 6 days of differentiation, cells with 3 days of differentiation and control cells. After the respective time points, 1 mL of PureZOL™ RNA Isolation Reagent (Trizol) was added to each well. The cellular extracts were collected to 1.5 mL microcentrifuge tubes and stored frozen at -20ºC until used. Next, 200 µL of Chloroform were added per 1 mL of Trizol (200 µL for each sample) followed by 2-3 minutes of shaking at room temperature. After, samples were centrifuged at 12 000xg for 15 minutes at 4ºC. This procedure resulted in a separation of RNA, DNA and Protein in three different phases (**Fig. 5**).

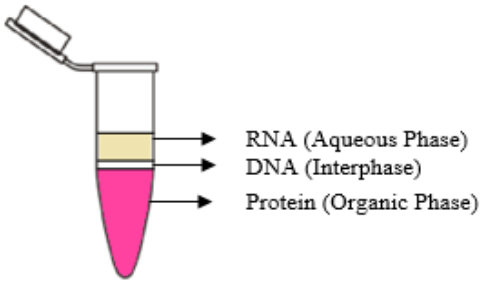

Figure 5. Trizol phase separation after chloroform addition.

After removing the Aqueous Phase 300 µL of 100% ethanol were added to the Organic Phase and Interphase followed by agitation for 2-3 minutes. Afterwards, samples were centrifuged at 2000xg for 5 minutes at 4ºC, resulting in formation of a pellet of DNA and a supernatant with protein. The supernatant was collected to a new microcentrifuge tube and 1.5 mL of isopropanol were added followed by a 10 minute incubation at room temperature to promote protein precipitation. Next, another centrifugation at 2000xg for 10 minutes at 4ºC was performed and supernatant was discarded.

The protein pellet was resuspended in 2 mL 0.3 M Guanidine Hydrochloride in 10% ethanol. After 20 minutes of incubation on ice the samples were centrifuged at 7500xg for 5 minutes at 4ºC and the supernatant was discarded. The last two steps were repeated twice and the final pellet was resuspended in 2 mL of 100% ethanol and vortexed. After 20 minutes of incubation at room temperature the samples were centrifuged at 7500xg for 5 minutes at 4ºC and the supernatant was discarded. Afterwards the pellet was air dried for 5 to 10 minutes and posteriorly dissolved in 1% SDS while heating at 50ºC. Finally the dissolved samples were centrifuged at 10 000xg for 10 minutes at 4ºC to remove non-solved material and the supernatant, containing the isolated protein, was collected.

3.5.2. Protein Quantification

The Bradford method was used to quantify the protein. This method consists in a colorimetric quantification that relies on an absorbance shift that occurs when the dye Coomassie Brilliant Blue G-250 binds to protein[113].

The protein samples were prepared with milli-Q water and buffer in which they were collected (1% SDS) and a standard curve was created with several dilutions of Bovine Serum Albumin (BSA) (**Table 2**). The Bradford Reagent was diluted in milli-Q water (1:5) and then added to the samples and standard curve just before absorbance measuring. All samples were performed in triplicates in a 96 multi-well plate and the absorbance was measured at 595 nm in Cytation™ 3 multiwell plate reader (BioTek Instruments, Winooski, VT, USA).

Table 2. Standard curve and sample preparation table for Bradford assay.

Protein (µg)	Milli-Q Water (µL)	0.1 % BSA (µL)	Collecting Buffer (µL)	Bradford Reagent (µL)
0 (blank)	79	0	1	120
1	78	1	1	120
2	77	2	1	120
3	76	3	1	120
4	75	4	1	120
5	74	5	1	120
		Sample (µL)		
Sample	79	1	-	120

3.5.3. Western Blot

After quantification, equal amounts of protein were diluted in Laemmli Blue Buffer 6 fold concentrated (1.88 mL of 1M Tris HCl, 0.63 g SDS, 7.9 mL Glycerol, and 0.003 g Bromophenol Blue to a final volume of 10 mL), supplemented with 0.3 M DTT. After, samples were heated at 95ºC for 5 minutes to promote protein denaturation. This sample preparation is a very important first step that allows protein separation to occur only depending on their molecular size by reducing disulphide S-S bonds formation and providing uniform negative charge to all proteins[114].

For the SDS-PAGE, and accordingly with the molecular weight of the proteins of interest, polyacrylamide gels were prepared. A total of 30 µg of protein was added to the gel. The protein separation was performed at room temperature with a constant amperage of 30 mA/gel until the bands reached the bottom end of the gel.

After electrophoresis, protein were transferred to a polyvinylidene difluoride (PVDF) membrane (Bio-Rad, Hercules, California, USA) through Trans-Blot® Turbo™ Transfer System (Bio-Rad, Hercules, California, USA) at a constant amperage of 1A for 20 minutes using Ready to Assemble Kit (Cat #170-4273 Bio-Rad, Hercules, California, USA). Once protein transfer was concluded the membranes were rinsed with distilled water and then stained with 0,5% Ponceau (diluted in 1% Glacial Acetic Acid). Ponceau is a reversible protein dyer that allowed to evaluate the transfer success confirming the protein loading[115]. The next step consisted in blocking the membrane to avoid non-specific protein binding during incubation with the primary antibody. The blocking was performed by incubation of the membrane with 15 ml of 5% dry milk diluted in TBS-T for 2 hours at room temperature with a constant shaking.

The primary antibodies (**Table 3**) were prepared in 2.5 ml of 1% dry milk in TBS-T. The membranes were incubated with primary antibody over night at 4ºC. After this the membranes were rinsed three times with TBS-T for 5 minutes and incubated with the respective secondary antibodies (**Table 4**) previously prepared in TBS-T. This last incubation was performed for 1 hour at room temperature with constant shaking. After incubation with secondary antibody, membranes were rinsed three times with TBS-T for 5 minutes each to remove the excess of secondary antibody.

Finally, Clarity Western ECL Substrate was added to the membranes. This substrate constitutes a chemiluminescent detection system since it generates light when oxidized by horseradish peroxidase (HRP), the enzymes conjugated with secondary antibodies[116]. After incubation, the protein bands in the membranes were visualized using the BioSpectrum® Imaging System™ (Cambridge, UK). Obtained images were processed in ImageJ software and bands densities were quantified using the Totallab TL120 Software.

Table 3. List of primary antibodies tested in Western Blot Analysis, respective molecular weights, chosen dilutions and companies from which they were obtained.

Primary Antibody	Molecular Weight	Dilution	Host Organism	Catalog Number	Company
Cathepsin K	43kDa	1:500	Mouse	sc-48353	Santa Cruz
Mitochondrial Superoxide Dismutase 2 (SOD2)	25kDa	1:500	Mouse	sc-133134	Santa Cruz
Total OXPHOS Cocktail	**CI**-NDUFB8: 20kDA **CII**-SDHB: 30kDa **CIII**-UQCRC2: 48kDa **CIV**-MTCO1: 40kDa **CV**-ATP5A: 55kDa	1:1000	Rodent	MS604	MitoScience

Table 4. List of secondary antibodies used in Western Blot Analysis, dilution and companies from which they were obtained.

Secondary Antibody	Dilution	Catalog Number	Company
Anti-mouse IgG, HRP-linked antibody	1:2000	7076P2	Cell Signaling

3.6. Mitochondrial DNA Copy Number Analysis

3.6.1. DNA Isolation and Quantification

For the present assay, RAW 264.7 cells were seeded in 6 well plate at a density of 15 625 cells/cm^2 and three main condition groups were established: cells with 6 days of differentiation, cells with 3 days of differentiation and control cells. After differentiation period cells were collected in culture medium using a cell scraper and centrifuged at 300xg for 5 minutes at room temperature. The resulting supernatant was discarded and the cellular pellet was resuspended in 200 µL of PBS.

DNA isolation was performed using QIAamp DNA Mini Kit (Qiagen, Hilden, Germany), following manufacturers' instructions. First, 20 µL of proteinase K were added to each sample followed by the addition of 200 µL of Buffer AL and a 15 seconds vortex to promote cellular lysis. Next, samples were incubated at 56ºC for 10 minutes to achieve a maximum DNA yield and briefly centrifuged to remove possible drops from the inside of the lid. Following this step 200 µL of molecular grade ethanol were added to each sample which were then vortexed for 15 seconds and briefly centrifuged for 5 seconds. The supernatant was transferred to QIAamp Mini Spin Columns, inserted on 2 mL collection tubes, and centrifuged at 6000xg for 1 minute at room temperature. After centrifugation the collection tubes were replaced by clean ones and the filtrate discarded. As a washing step, 500 µL of Buffer AW1 were added to the spin columns followed by another centrifugation as 6000xg for 1 minute at room temperature and the resulting filtrate was again discarded. Next, 500 µL of Buffer AW2 were added to the columns and centrifuged at 20000xg for 3 minutes at room temperature. The obtained filtrate was discarded and the QIAamp Mini Spin Columns were placed in clean 1.5 mL microcentrifuge tubes. For the elution step, 200 µL of Buffer AE were added to the spin columns followed by a 5 minute incubation at room temperature to increase DNA yield and a final centrifugation at 6000xg for 1 minute at room temperature. The filtrate has the purified DNA.

DNA was quantified using NanoDrop 2000 (ThermoScientific, Waltham, MA, USA) measuring the sample absorbance at 260 nm. The ratio between the readings at 260 nm and 280 nm (A_{260}/ A_{280}) allowed to obtain an estimate of DNA purity. All samples with a ratio between 1.8 and 2.0 were considered pure and used for DNA copy number assessment.

3.6.2. DNA Copy Number Assessment

Mitochondrial DNA copy number was assessed by quantitative Real Time Polymerase Chain Reaction (qRT-PCR). DNA samples were diluted in DNase/ RNase free water to a final concentration of 10 ng/mL and plated in a Hard-Shell PCR 96-well plate along with the tested primers, DNase/ RNase free water and EvaGreen Supermix for the target sequence amplification. Each well contained a final volume of 10 µL in which were included 2.5 µL of the DNA sample, performing a total of 25ng of DNA per well, 0.5 µL of each tested primer, both forward and reverse, 2.4 µL of DNase/ RNase free water and 5 µL of EvaGreen Supermix. The used primers and their correspondent forward and reverse sequences are presented in **Table 5.**

Table 5. List of primers for mitochondrial and nuclear reference genes used for Real Time Polymerase Chain Reaction (qRT-PCR).

Gene	Designation	DNA	Forward Primer	Reverse Primer
Nd1	NADH-ubiquinone oxidoreductase core subunit 1	Mitochondrial	GGCCCATTCGCGTTATTCTTT	GATCGTAACGGAAGCGTGGA
ApoB	Apolipoprotein B	Nuclear	TCCCACGTAGAACCCGTTTG	AGTCTCATCGCTACCCCACT

DNase/ RNase free water replaced the DNA sample in the negative control wells designated No Template Controls (NTC). Additionally, pools from all samples were diluted in DNase/ RNase free water in ratios from 1:1, 1:10 and 1:100 to create efficiency curves for each set of primers.

The PCR reaction was performed using Bio-Rad® CFX96™ Real Time PCR system (Bio-Rad, Hercules, CA, USA) accordingly to the protocol represented in **Fig. 6**. Using the B2m gene as

reference, the relative normalized expression was determined by Bio-Rad® CFX96 Manager software (version 3.1) (Bio-Rad Laboratories, Hercules, California, USA).

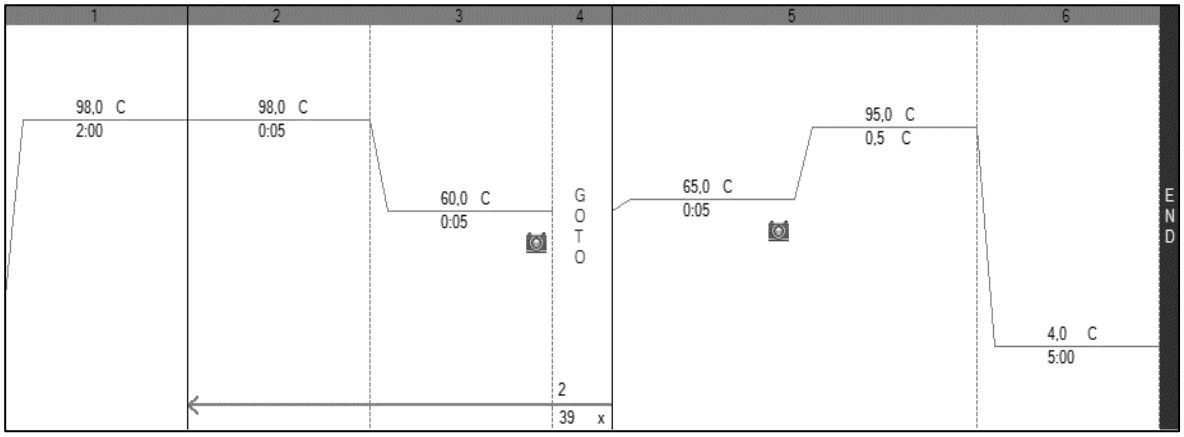

Figure 6. Bio-Rad optimized PCR protocol. The first step consists in an increase of temperature to 98ºC promoting DNA polymerase activation. The second and third steps compose a full cycle where DNA is fully denaturated allowing the primer annealing when temperature decreases to 60ºC. This cycle repeats for a total of 40 times and after that, the melting temperature of the PCR products is determined when temperature increased from 65ºC to 95ºC. The reaction stops when the temperature drops to 4ºC in the final step.

3.7. Fluorescence-based assays

3.7.1. Intracellular Reactive Oxygen Species (ROS)

Intracellular ROS production was measured using the CM-H_2DCFDA probe. Once inside the cell, CM-H_2DCFDA is cleaved by intracellular esterases resulting in a non-fluorescent molecule (H_2DCF). This molecule, upon ROS oxidation, gets converted into 2',7'-dichlorofluorescein (DCF) which is highly fluorescent. The fluorescence measurement allows evaluating cellular ROS production[117].

This assay was performed in two different ways varying in cell culture conditions and differentiation time periods:

i) RAW 264.7 cells were seeded in a 96-well clear bottom black side plate at a density of 15 625 cells/cm^2 and after two days of growth, differentiation was induced upon exposure to 50 ng/mL of RANKL for 6 days. Undifferentiated cells were used as control.

ii) RAW 264.7 cells were seeded in a 96-well clear bottom black side plate at a density of 15 625 cells/cm^2 and two days after the seeding the regular culture medium was replaced with Charcoal Stripped Culture Medium containing the respective cells treatments: 50 ng/mL of RANKL; 10 nM of Estradiol; 50 ng/mL of RANKL plus 10 nM Estradiol; 10 nM of MPP; 50 ng/mL of RANKL plus 10 nM MPP; 10 nM of PHTPP; and 50 ng/mL of RANKL plus 10 nM PHTPP. MPP and PHTPP are specific antagonists for Estrogen Receptor Alpha and Estrogen Receptor Beta, respectively[104]. They were used in this assay as an attempt to understand the relation between estrogen receptors and the osteoclast differentiation process as well as their impact on intracellular ROS production. Cells remained in these culture conditions for 6 hours and 24 hours before the H_2DCFDA fluorescence reading assay.

Before the assay DMEM was supplemented with 25 mM Glucose, 4 mM Glutamine, 1 mM Sodium Pyruvate, 5 mM of HEPES and the pH was set to 7,4. CM-H_2DCFDA was added at a final concentration of 5µM. After treatment cells were incubated with DMEM medium supplemented with 5 µM CM-H_2DCFDA for 45 minutes at 37ºC in the dark. Undifferentiated RAW 264.7 cells, treated for 15 minutes with 10 mM of Hydrogen Peroxide Solution (H_2O_2) were used as a positive control group. Following, the medium was replaced by supplemented DMEM without the probe and fluorescence was read between 485 nm and 528 nm in Cytation™ 3 multi-well plate reader (BioTek

Instruments, Winooski, VT, USA). At the end of the reading cells were fixed overnight with 10% trichloroacetic acid (TCA) at 4ºC for further normalization.

3.7.2. Mitochondrial Reactive Oxygen Species (ROS)

Mitochondrial ROS production was measured using MitoSOX Red dye. Due to its positive charge, this dye targets the mitochondrial matrix where it is oxidized by superoxide. The product of this reaction emits fluorescence at 580 nm, after being excited at 510 nm, allowing to assess mitochondrial ROS production[118].

For this assay RAW 264.7 cells were seeded in a 96-well clear bottom black side plate at a density of 15 625 cells/cm^2 and after two days of growth, differentiation was induced upon exposure to 50 ng/mL of RANKL for 6 days. Undifferentiated cells were used as control.

At the day of the assay, DMEM was supplemented with 25 mM Glucose, 4 mM Glutamine, 1 mM Sodium Pyruvate, 5 mM of HEPES and the pH was set to 7,4. MitoSOX Red was added to the supplemented medium at a final concentration of 5 µM. After treatment, the culture medium was removed and replaced by fresh medium supplemented with 5 µM of MitoSOX. Cells were incubated with MitoSOX for 30 minutes at 37ºC in the dark. Undifferentiated RAW 264.7 cells incubated with 2 µM of Antimycin were used as the positive control group. After the incubation period fluorescence was read between 510 nm and 580 nm in Cytation™ 3 plate reader (BioTek Instruments, Winooski, VT, USA). The reading was performed for a total of 180 minutes with intervals of 2 minutes between measurements. Following, cells were fixed overnight with 10% TCA at 4ºC, for further normalization.

3.7.3. Evaluation of Cell Density by Sulforhodamine B (SRB) assay

Sulforhodamine B is a bright-pink dye with the ability to bind protein due to the presence of two sulfonic groups in its composition. These groups allow the compound to bind basic amino acid residues under acidic conditions and dissociate them under basic conditions. This characteristic allows the performance of a colorimetric method relying on proportion between the intensity of SRB staining and the cellular mass[119].

Sulforhodamine B assay was used as a normalization procedure and therefore it was performed after the indicated assays on previously fixed cells. 50 µL of 0.05% SRB diluted in 1% acetic acid were added to each well and the plate was incubated for 30 minutes in the dark at room temperature. After incubation, the wells were washed with 1% acetic acid to remove all of the unbound dye and dried at 37ºC. Finally, the bound dye was solubilized in 200 µL of 10 mM Tris pH 10 and half of that volume was transferred to a new plate. Optical density was determined at 530 nm in Cytation™ 3 plate reader (BioTek Instruments, Winooski, VT, USA).

3.8. Extracellular flux analysis to measure Mitochondrial Oxygen Consumption Rate and Extracellular Acidification Rate

Mitochondrial activity was evaluated by measuring oxygen consumption rate (OCR) and extracellular acidification rate (ECAR) using the Seahorse XFe96 Extracellular Flux Analyzer. These measurements are key indicators that allow to assess mitochondrial respiration and glycolysis, respectively.

This test was performed in three different ways varying in cell culture conditions and differentiation time periods:

i) RAW 264.7 cells were seeded in a Seahorse XFe96 Cell Culture Microplate at an optimized density of 5000 cells per well. Differentiation was induced upon exposure to 50 ng/mL of RANKL for 1, 3 and 6 days. Undifferentiated cells were used as control.

ii) RAW 264.7 cells were seeded in a Seahorse XFe96 Cell Culture Microplate at an optimized density of 5000 cells per well two days before the Mito Stress assay to perform an acute effect study with 50 ng/mL of RANKL, 100 nM of Estradiol and 1 µM of Estradiol.

iii) RAW 264.7 cells were seeded in a Seahorse XFe96 Cell Culture Microplate at an optimized density of 5000 cells per well. After two days in culture, the culture media was replaced by several different conditions: 50 ng/mL of RANKL in Charcoal Stripped Culture Medium; 10 nM of Estradiol in Charcoal Stripped Culture Medium; and 50 ng/mL of RANKL plus 10 nM of Estradiol in Charcoal Stripped Culture Medium. Cells remained in these culture conditions for three different time periods: 1 hour, 24 hours and 48 hours. Undifferentiated RAW 264.7 cells cultured in Charcoal Stripped Culture Medium were used as control.

In the day prior to each assay, the Seahorse XFe96 sensor cartridge was hydrated by adding 200 µL per well of milli-Q water and left overnight at 37ºC in an incubator without CO_2.

At the day of the assay, the milli-Q water was removed from the cartridge and replaced by 200 µL of Seahorse XF Calibrant. After this the cartridge remained for about 1 hour in the incubator before loading the assay solutions. During this period of time, 100 mL of DMEM supplemented with 25 mM Glucose, 4 mM Glutamine, 1 mM Sodium Pyruvate, 5 mM of HEPES and pH 7,4 were prepared. Next, all culture conditions to which cells were previously submitted were prepared in this medium for the time of the assay. The cell plate was then carefully rinsed three times with assay

medium and the prepared conditions were added to the respective wells. This step was followed by an incubation of the cell plate at 37ºC without CO_2.

Oligomycin, Carbonyl cyanide-4 (trifluoromethoxy) phenylhydrazone (FCCP), and Rotenone plus Antimycin A constituted the compounds that were injected during the assay.

Oligomycin is an inhibitor of the F_O subunit of ATP synthase, also known as Complex V of the Mitochondrial Respiratory Chain. ATP synthase is responsible for ATP generation as a result of proton flux, though the F_O subunit, to the mitochondrial matrix. Its inhibition with Oligomycin allows to observe proton passage through the mitochondrial inner membrane that is not dependent on this complex and therefore this condition is called proton leak (**Fig. 7**)[120]. On other hand, FCCP is an uncoupling agent that disrupts the proton gradient by allowing them to pass through the mitochondrial inner membrane independently of ATP synthase. This will disrupt mitochondrial membrane potential leading to an increased electron transport that results in maximal oxygen consumption rate as an attempt to restore it (**Fig. 7**)[121].

Rotenone and Antimycin A are inhibitors of Mitochondrial Respiratory Chain Complex I and Complex III, respectively. The combined injection of both stops mitochondrial respiration[122].

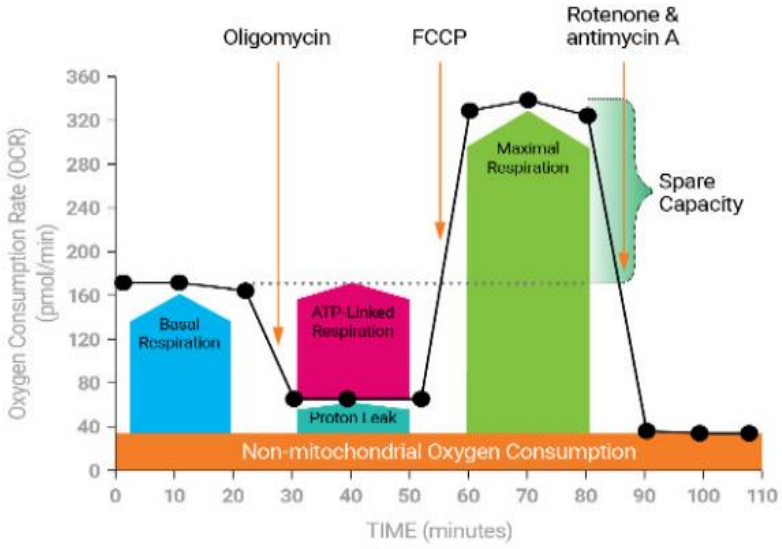

Figure 7. Representative scheme of measured parameters in a Seahorse XF Cell Mito Stress Test: basal respiratory rate, ATP-linked oxygen consumption, proton leak, maximal respiration, spare respiratory capacity and non-mitochondrial respiration. Figure obtained from Agilent Website (Agilent Technologies, Santa Clara, California, USA).

In addition to these compounds, in the acute study situation, 50 ng/mL of RANKL, 100 nM and 1 µM of Estradiol were the first injected compounds.

Optimized final concentrations of 3 µM Oligomycin, 0.25 µM FCCP, and 2 µM Rotenone plus 2 µM of Antimycin A were prepared in assay medium taking into account the volume already present in the plate wells. Next, the prepared solutions were loaded into the cartridge through doors A, B and C respectively. In the acute study, door A corresponded to the acute injection of RANKL and Estradiol, and doors B, C and D contained Oligomycin, FCCP and Rotenone/ Antimycin A, respectively. The injection volume was 25 µL per well.

The assay began by inserting the cartridge with Seahorse XF Calibrant in the Seahorse XFe96 Analyzer (Agilent Technologies, Santa Clara, California, USA). In this step, calibration was performed and the wells oxygen conditions and pH were verified through the cartridge sensors that stayed inserted in the wells during the following experiment. Finally, after calibration completion the plate containing Seahorse XF Calibrant was expelled and replaced by the cell plate. The used protocol was previously defined using Wave 2.6 Software (Agilent Technologies, Santa Clara, California, USA). At the end of the assay, cells were fixed with 10% TCA at 4ºC for further normalization.

3.9. Statistical Analysis

All data analysis was performed using GraphPad Prism 6.0 program and presented as mean value ± SEM for the number of experiments indicated in the legends of the figures presented in the results chapter. Kruskal Wallis non-parametric test was used to perform statistical analysis, followed

by Dunn's multiple comparison test. In exceptional cases where the resultant data presented a normal distribution, the parametric T test was used to perform statistical analysis. In both cases significance was accepted with p value < 0.05.

4. RESULTS

4.1. RAW 264.7 differentiation into osteoclasts and characterization of differentiated cells

4.1.1. Expression of mature osteoclast markers

TRAP and cathepsin K are two examples of already described osteoclasts hallmark proteins that are involved in bone resorption and, therefore, are indicators of osteoclast activity. TRAP is a glycoprotein involved in the migration of active osteoclasts to the resorption site[123]. Cathepsin K on its turn, it's a protease capable of catabolizing collagen and therefore it is directly involved in bone matrix degradation[124].

In this chapter, we aimed to confirm RAW 264.7 macrophages differentiation into osteoclasts upon 6 days exposure to 50 ng/mL of RANKL and quantify the percentage of obtained mature osteoclasts after this period. For this purpose TRAP and cathepsin K were the selected differentiation markers.

At day 6 of exposure to RANKL, it was possible to observe that cells presented a darker color when compared to the controls, being considered TRAP positive (**Fig. 8A**). This color occurs as a result of TRAP catalytic activity upon the addition of its substrate, present in the TRAP staining kit (naphthol_AS_BI phosphate). The dark staining along with the presence of 3 or more nuclei were the two criteria used to consider differentiated cells as mature and active osteoclasts. In our experimental conditions, a total of 2.7% of cells were classified as fully differentiated osteoclast after 6 days exposure to RANKL.

Regarding cathepsin K, although no significant differences were observed when the statistical analysis was performed, Western Blot results showed an apparent increase in this protein content at

day 3 and day 6 of differentiation when compared to control, decreasing from day 3 to day 6 (**Fig. 8B**).

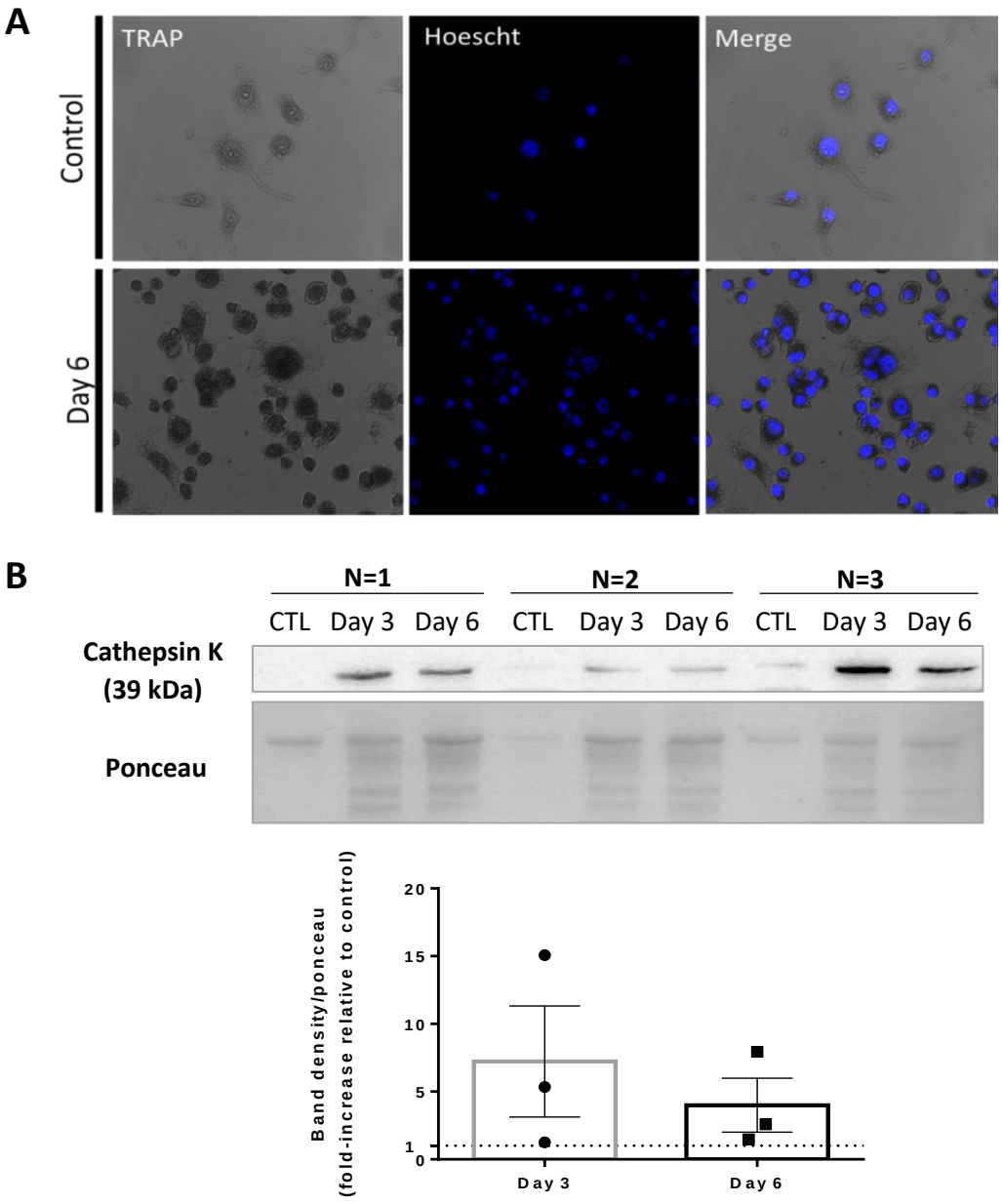

Figure 8. RAW 264.7 expression of mature osteoclast markers after exposure to RANKL. A) Fluorescent microscopy images of RAW 264.7 stained for Tartrate Resistant Acid Phosphatase (TRAP) and Hoescht before and after 6 days differentiation upon exposure to 50 ng/mL of RANKL. TRAP positive cells with 3 or more nuclei were considered mature osteoclasts. Images are representative of 3 independent experiments and were obtained by epi-fluorescence microscopy using a 40x objective with numerical aperture 0.60. **B)** Western Blot analysis of cathepsin K levels in control cells and cells exposed to 50 ng/mL of RANKL for 3 and 6 days. Images and band density quantification are representative of 3 independent experiments. Graph

bars are presented as fold-increase relative to the control and showed as mean ±SEM. Ponceau S was used as loading control.

In addition, it is important to refer that Ponceau was used to normalize Western Blot results. This technique was preferred over the use of a housekeeping protein since the last one could be affected by the differentiation process which implies cellular morphology alterations.

4.1.2. Analysis of mitochondrial bioenergetics during RAW 264.7 differentiation into osteoclast

There are several lines of evidence that show a relation between mitochondrial activity and osteoclastogenesis[121]. Previous studies consider that the presence of intact and active mitochondria is crucial for osteoclast differentiation as well as bone matrix resorption activity. They highlight that there are several alterations in mitochondrial functioning, for example in mitochondrial respiration, that occur during the differentiation process[122].

Taking these findings into account we measured oxygen consumption rate and extracellular acidification rate using the Seahorse XFe96 Extracellular Flux Analyzer to assess mitochondrial respiration during osteoclast differentiation. OCR-associated parameters such as basal and maximal respiration, ATP-linked oxygen consumption, proton leak and spare respiratory capacity, decreased along differentiation when compared to the control (**Fig. 9A**). As the period of exposure to RANKL increases, cell oxygen consumption decreases significantly from day 1 to day 3 and day 6 of differentiation. Additionally, the decrease observed in extracellular acidification rate during differentiation (**Fig. 9B**) allowed us to conclude that RANKL seems to induce a decrease in cellular metabolic activity, with cell acquiring a more quiescent profile after 3 and 6 days exposure to RANKL.

A

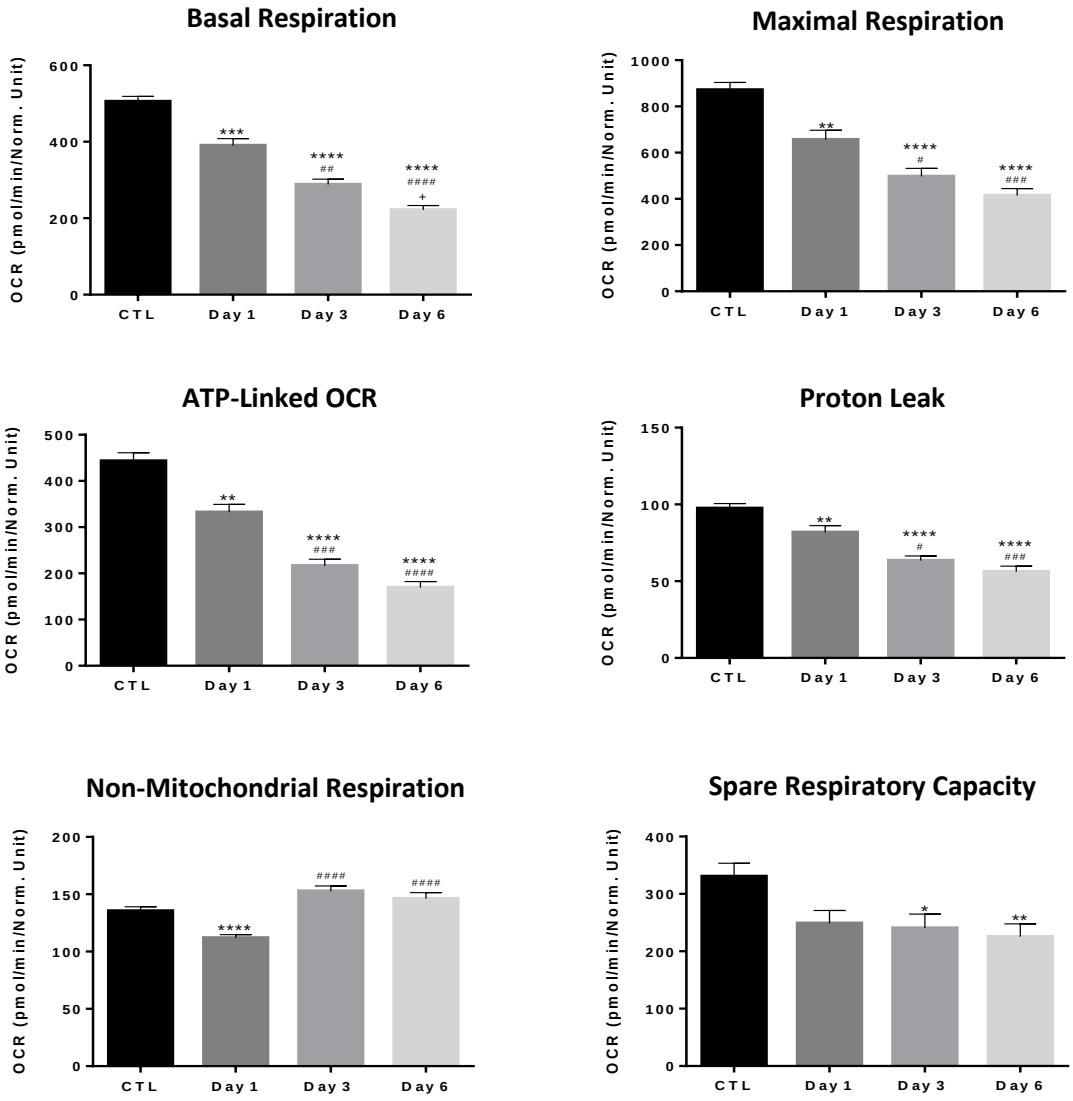
Basal Respiration
OCR (pmol/min/Norm. Unit)
600
400
200
0
***
****
##
****
####
+
CTL
Day 1
Day 3
Day 6
Maximal Respiration
OCR (pmol/min/Norm. Unit)
1000
800
600
400
200
0
**
****
#
****
###
CTL
Day 1
Day 3
Day 6
ATP-Linked OCR
OCR (pmol/min/Norm. Unit)
500
400
300
200
100
0
**
****
###
****
####
CTL
Day 1
Day 3
Day 6
Proton Leak
OCR (pmol/min/Norm. Unit)
150
100
50
0
**
****
#
****
###
CTL
Day 1
Day 3
Day 6
Non-Mitochondrial Respiration
OCR (pmol/min/Norm. Unit)
200
150
100
50
0
****
####
####
CTL
Day 1
Day 3
Day 6
Spare Respiratory Capacity
OCR (pmol/min/Norm. Unit)
400
300
200
100
0
*
**
CTL
Day 1
Day 3
Day 6

B

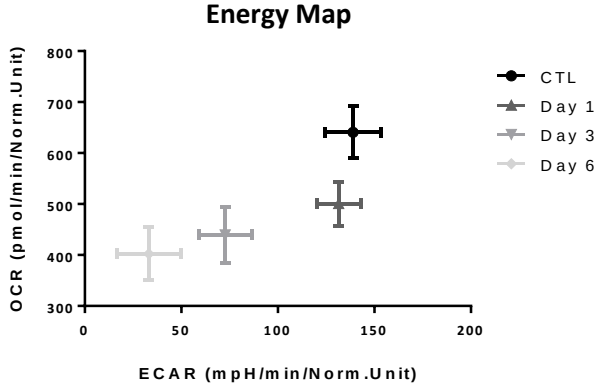
Energy Map
OCR (pmol/min/Norm.Unit)
800
700
600
500
400
300
0
50
100
150
200
ECAR (mpH/min/Norm.Unit)
CTL
Day 1
Day 3
Day 6

Figure 9. Mitochondrial respiratory parameters of RAW 264.7 cells exposed to 50 ng/mL of RANKL for 1, 3 and 6 days. A) Basal respiration, maximal respiration, ATP-linked oxygen consumption rate, proton leak, non-mitochondrial respiration and spare respiratory capacity. **B)** Oxygen consumption rate (OCR) versus extracellular acidification rate (ECAR) during exposure of RAW 264.7 cells to RANKL. All data are presented as mean ±SEM of 12 replicates of 5 independent experiments. SRB technique was used for normalize the obtained data.*P < 0.05; **P < 0.01, ***P < 0.001 and ****P < 0.0001, when compared to the control. $^{\#}$P < 0.05; $^{\#\#}$P < 0.01, $^{\#\#\#}$P < 0.001 and $^{\#\#\#\#}$ P < 0.0001, when compared to Day 1. $^{+}$P < 0.05 when compared to Day 3.

4.1.2.1. Alterations in mitochondrial electron transport chain complexes during RAW 264.7 differentiation into osteoclasts

Taking into account the results obtained in the previous chapter we proceeded to the analysis of protein expression levels of Complex I, Complex II, Complex III, Complex IV and ATP synthase of the mitochondrial electron transport chain in RAW 264.7 cells exposed to 50 ng/mL of RANKL for 3 days and 6 days compared to control cells. We relied on the fact that a decrease in complexes expression levels might be in the origin of a possible explanation for diminished oxidative phosphorylation in cells exposed to RANKL. Despite that, it is possible to observe an apparent increase in the protein levels of Complex II, Complex III, Complex IV and ATP synthase in cells exposed to RANKL when compared to RAW 264.7 control cells, especially in the third day of differentiation. Although, no significant differences were observed (**Fig.10**). Regarding Complex I, it was not possible to distinguish the correspondent protein band due to the presence of unspecific antibody binding in the membrane area correspondent to this protein molecular weight.

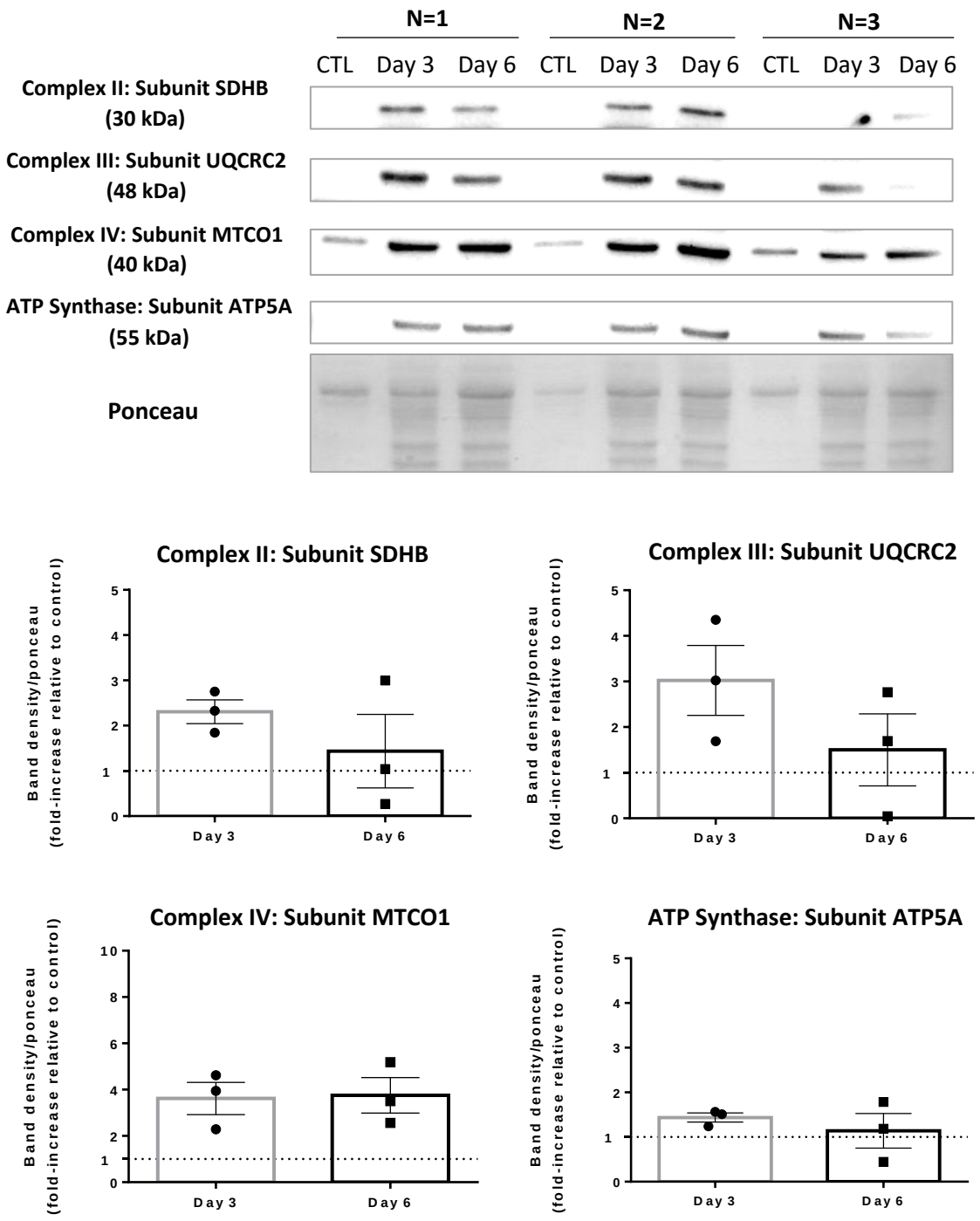

Figure 10. Alterations in the protein levels of mitochondrial Complex II, Complex III, Complex IV, and ATP synthase in control RAW 264.7 cells and cells exposed to 50 ng/mL of RANKL for 3 days and 6 days. Images and band density quantification are representative of 3 independent experiments. Graph bars are presented as fold-increase relative to the control and showed as mean ±SEM. Ponceau S was used as loading control.

4.1.2.2. Alterations in mitochondrial DNA copy number during RAW 264.7 differentiation into osteoclasts

An altered mitochondrial DNA (mtDNA) copy number is many times in the origin of several diseases appearance. Defects in genes responsible for mitochondrial DNA biogenesis and for the maintenance of its integrity can lead to a reduced DNA copy number in the cell. Additionally, mtDNA encodes several subunits of Complex I, Complex III, Complex IV and ATP synthase being essential for oxidative phosphorylation. Therefore if mtDNA is somehow compromised, mitochondrial metabolic function may be impaired[127].

Taking into account that previous chapter results were not statistically significant, DNA copy number was assessed as an attempt to find a cause for the observed decrease in oxidative phosphorylation after RANKL exposure for 3 days and 6 days. Regarding this experiment, no significant results were obtained, which can be explained by the low number of independent experiments (2 replicates of 2 independent experiments). However, the mean value of the ratio mtDNA/nDNA appears to increase at day 3 and day 6 of exposure to 50 ng/mL of RANKL when compared to the control (**Fig. 11**).

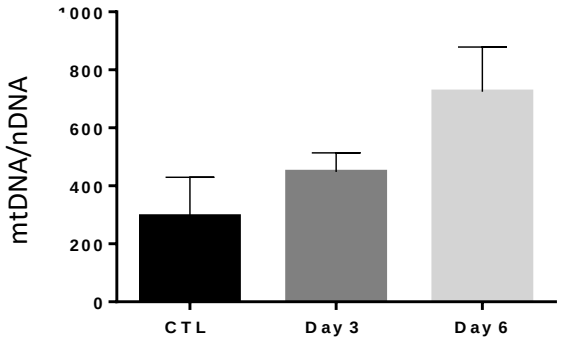

Figure 11. MtDNA copy number content in RAW 264.7 control cells and RAW 264.7 exposed to 50 ng/mL of RANKL for 3 and 6 days. mtDNA copy number was measured by quantifying Nd1 expression, normalized to ApoB expression levels. Data are represented as mean ±SEM of 2 replicates of 2 independent experiments.

4.1.3. Cellular and mitochondrial ROS production during RAW 264.7 differentiation into osteoclasts

There are several lines of evidence showing that ROS production is a key factor in RANKL-mediated osteoclast differentiation presenting ROS as important second messengers for its occurrence[128]. Taking these findings into consideration, we aimed to assess changes in both cellular and mitochondrial ROS production after RAW 264.7 cells being exposed to RANKL for 6 days. Moreover, focusing on mitochondrial ROS production, SOD2 expression was also evaluated since there is evidence showing that its expression can be increased by RANKL action[58]. This enzyme is responsible for reducing superoxide radicals in mitochondria converting them to hydrogen peroxide.

The obtained results show a significant increase both in cellular and mitochondrial ROS production after 6 days of exposure to 50 ng/mL of RANKL when compared to the control (**Fig. 12A, B**). Regarding SOD2, no significant statistical differences were observed in the Western Blot results. (**Fig. 12C**).

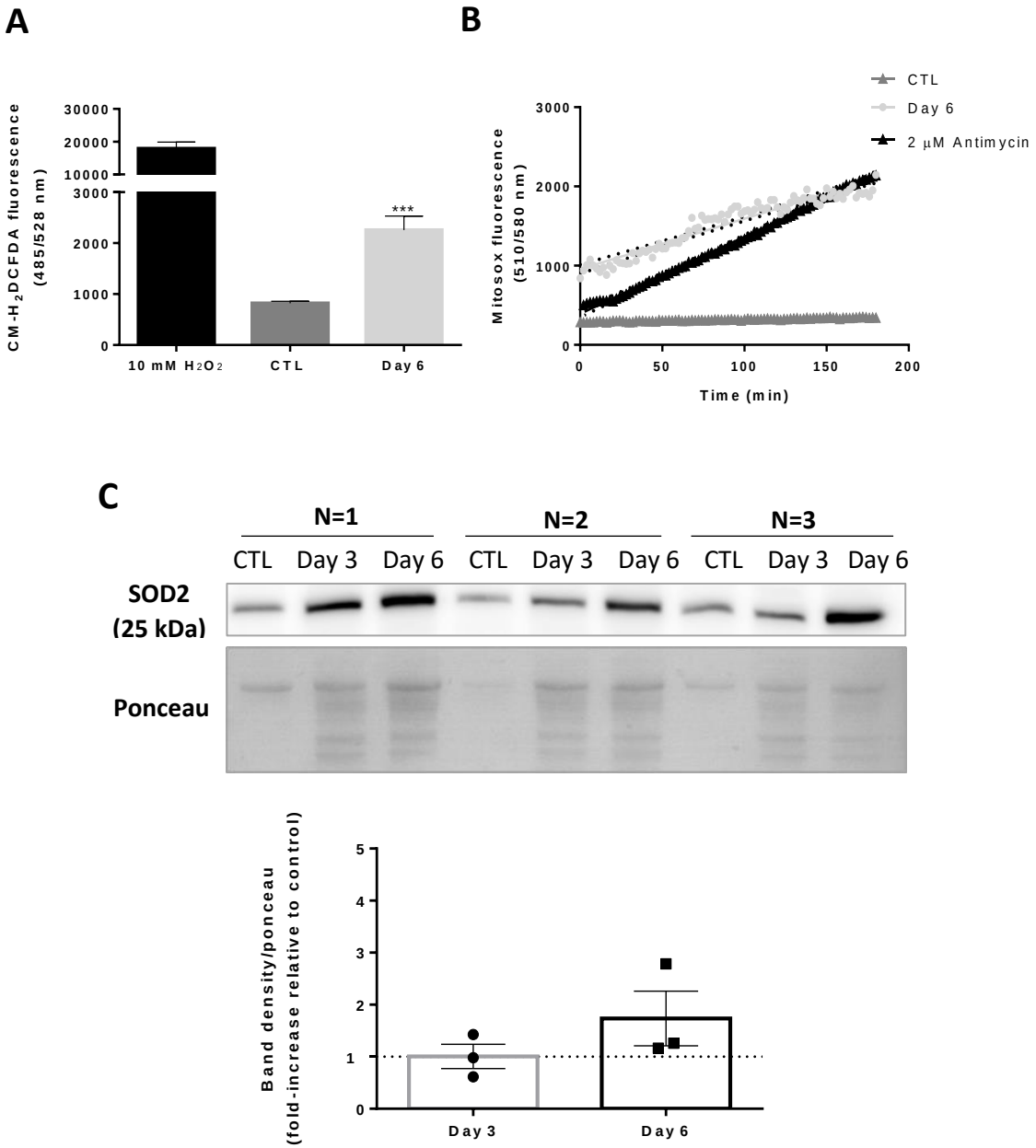

Figure 12. Cellular and mitochondrial ROS production during RAW 264.7 macrophages differentiation into osteoclasts. A) Cellular ROS production of RAW 264.7 cells exposed to 50 ng/mL of RANKL for 6 days. ROS measurement was performed using CM-H_2DCFDA probe and RAW 264.7 cells treated with 10 mM of H_2O_2 were used as a positive control. Data are presented as mean ±SEM of 8 replicates of 2 independent experiments. SRB technique was used as normalization procedure. *P < 0.05, **P < 0.01 and ***P < 0.001, when compared to the control. **B)** Mitochondrial ROS production of RAW 264.7 cells exposed to 50 ng/mL of RANKL for 6 days. ROS measurement was performed using MitoSOX probe and RAW 264.7 macrophages treated with 2 µM of Antimycin were used as positive control. Fluorescence emission reading

was performed for 180 minutes with intervals of 2 minutes between readings. Data are presented as mean with an interval of 95% confidence. SRB technique was used as normalization procedure. **C)** Western Blot analysis of SOD2 expression in control cells and cells exposed to 50 ng/mL of RANKL for 3 and 6 days. Images and band density quantification are representative of 3 independent experiments. Graph bars are presented as fold-increase relative to the control and showed as mean ±SEM. Ponceau S was used as loading control.

4.2. Acute effect of RANKL and 17β-estradiol (E2) on metabolic profile of RAW 264.7 macrophages

The direct effect of RANKL and E2 on metabolic profile of RAW 264.7 macrophages was evaluated using the Seahorse XFe96 Extracellular Flux Analyzer to measure the oxygen consumption and the extracellular acidification rates. For this experiment, two different E2 concentrations (100 nM and 1 μM) were tested.

The results obtained from this analysis demonstrate that acute treatment with 50 ng/mL of RANKL increased the oxygen consumption of RAW 264.7 macrophages (**Fig. 13**). No significant differences were observed in this parameter regarding both concentrations of E2. However, 30 minutes after acute injection with 100 nM and 1μM of E2 lead to an increase in ATP-linked and proton leak-linked OCR (**Fig. 13**). Apart from the acute response, acute injection of 50 ng/mL of RANKL did not imply a significant alteration in RAW 264.7 mitochondrial respiration profile. Additionally, no significant differences were observed in maximal respiration, non-mitochondrial respiration and spare respiratory capacity after RANKL or E2 acute injections.

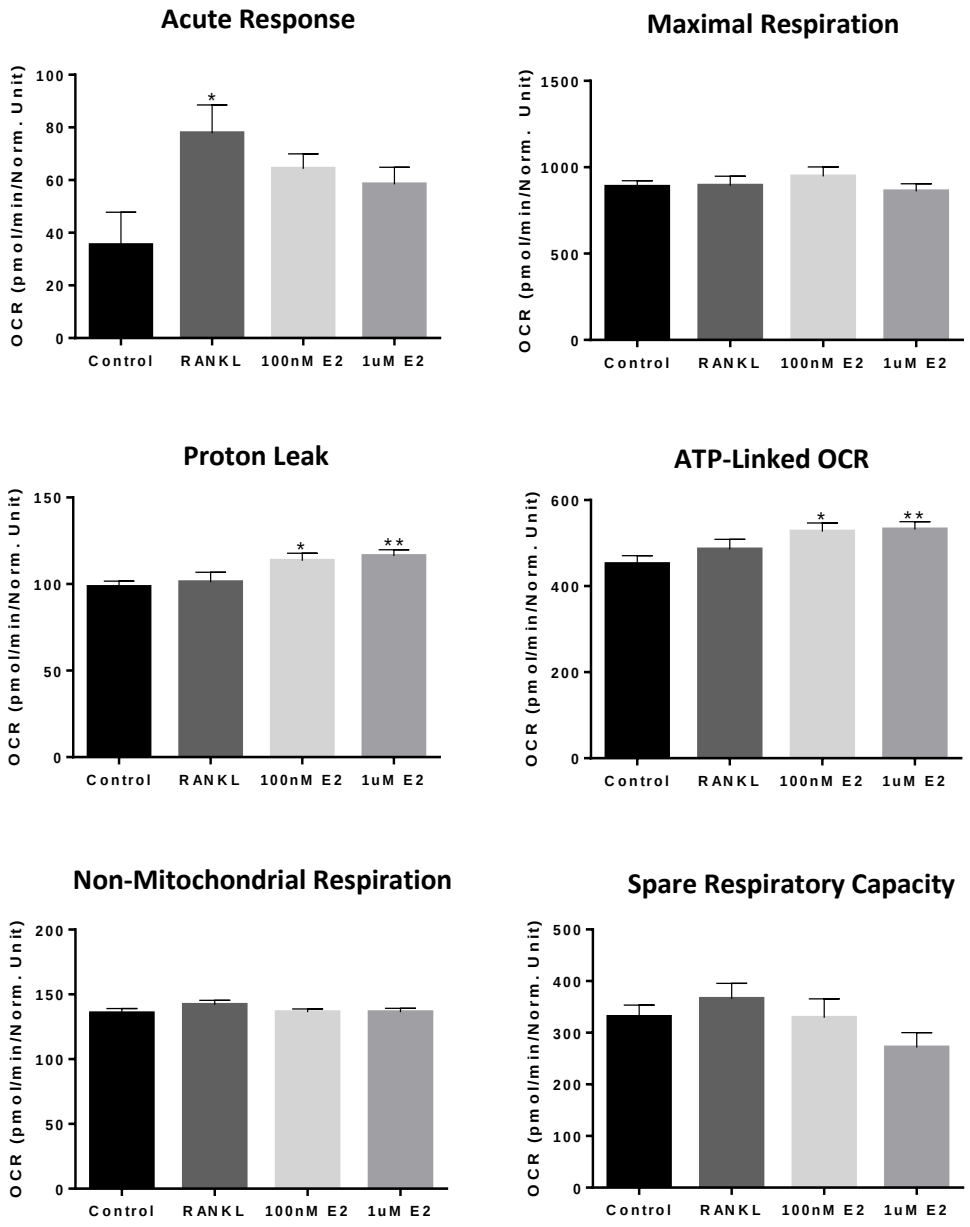

Figure 13. Mitochondrial respiratory parameters of RAW 264.7 macrophages after acute exposure to 50 ng/mL of RANKL, 100 nM of E2 and 1µM of E2. Basal respiration, maximal respiration, ATP-linked oxygen consumption rate, proton leak, non-mitochondrial respiration and spare respiratory capacity of RAW 264.7 cells during acute exposure to 50 ng/mL of RANKL, 100 nM of E2 and 1 µM of E2. All data are presented as mean ±SEM of 12 replicates of 5 independent experiments. SRB technique was used for normalizing the obtained data.*$P < 0.05$; **$P < 0.01$, when compared to the control.

4.3. RANKL and estrogen impact on mitochondrial respiration of RAW 264.7 macrophages differentiated in charcoal stripped medium

Given that estrogen has an inhibitory effect on RANKL-induced osteoclast differentiation, in this chapter, we aimed to understand what happens to mitochondrial respiration of RAW 264.7 macrophages when they are differentiated through exposure to RANKL in the presence of E2. For this purpose, culture medium supplemented with charcoal stripped FBS was used, to avoid the interference of estrogens normally present in FBS in the obtained results. To perform this assay, 10 nM of E2 were used as it represents the nearest concentration of estrogen at physiological levels.

Additionally, for this experiment, the incubation time with RANKL and E2 was 1h, 24h, and 48h. This relied on the observation of the previous results, in chapters **4.1.1.** and **4.1.2.**, where it was demonstrated that RAW 264.7 macrophages already show alterations in their metabolism and protein expression at an early stage of the differentiation process.

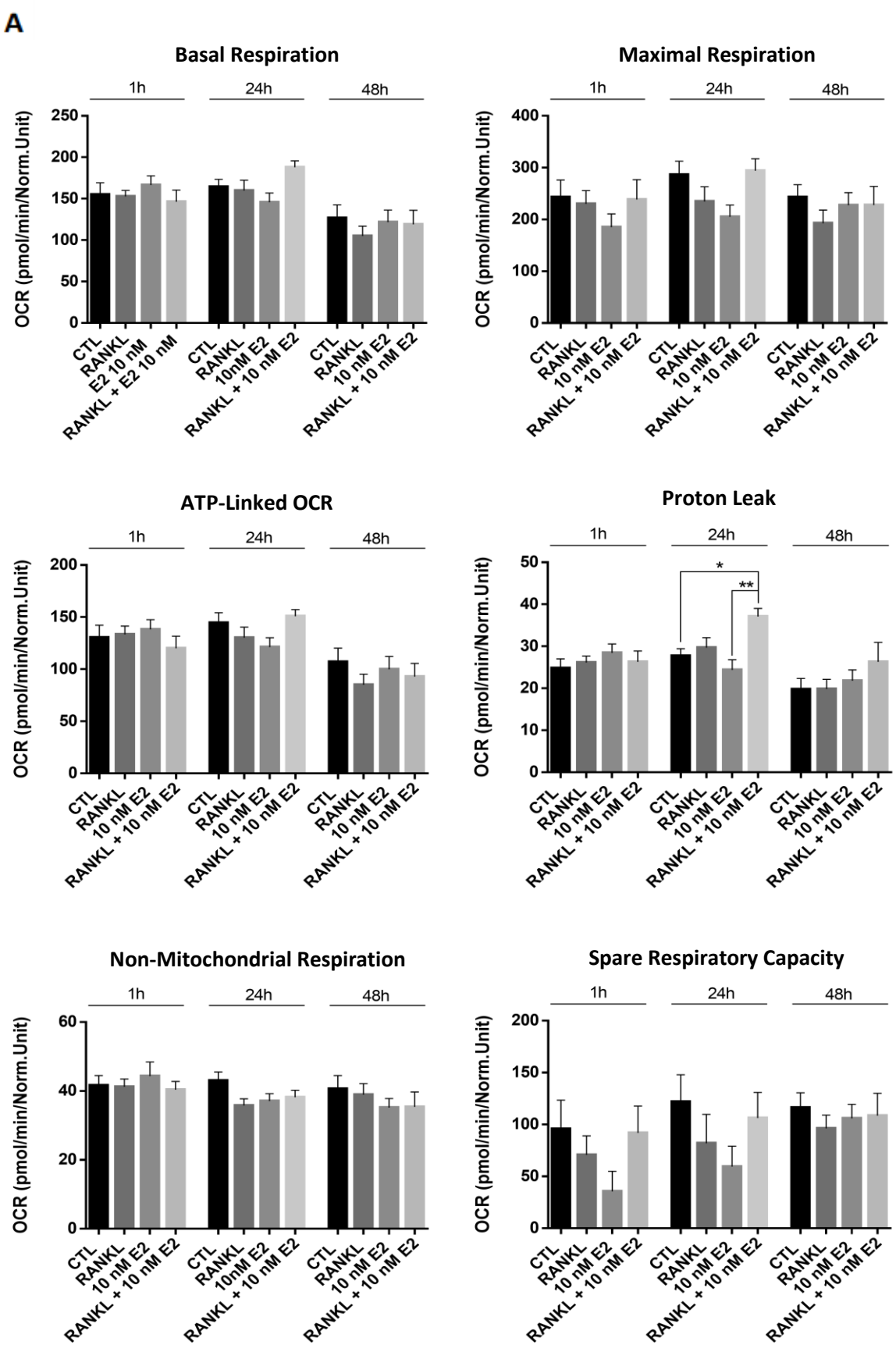
A
Basal Respiration
Maximal Respiration
ATP-Linked OCR
Proton Leak
Non-Mitochondrial Respiration
Spare Respiratory Capacity
1h
24h
48h
OCR (pmol/min/Norm.Unit)
CTL
RANKL
E2 10 nM
RANKL + E2 10 nM
10nM E2
10 nM E2
RANKL + 10 nM E2
*
**

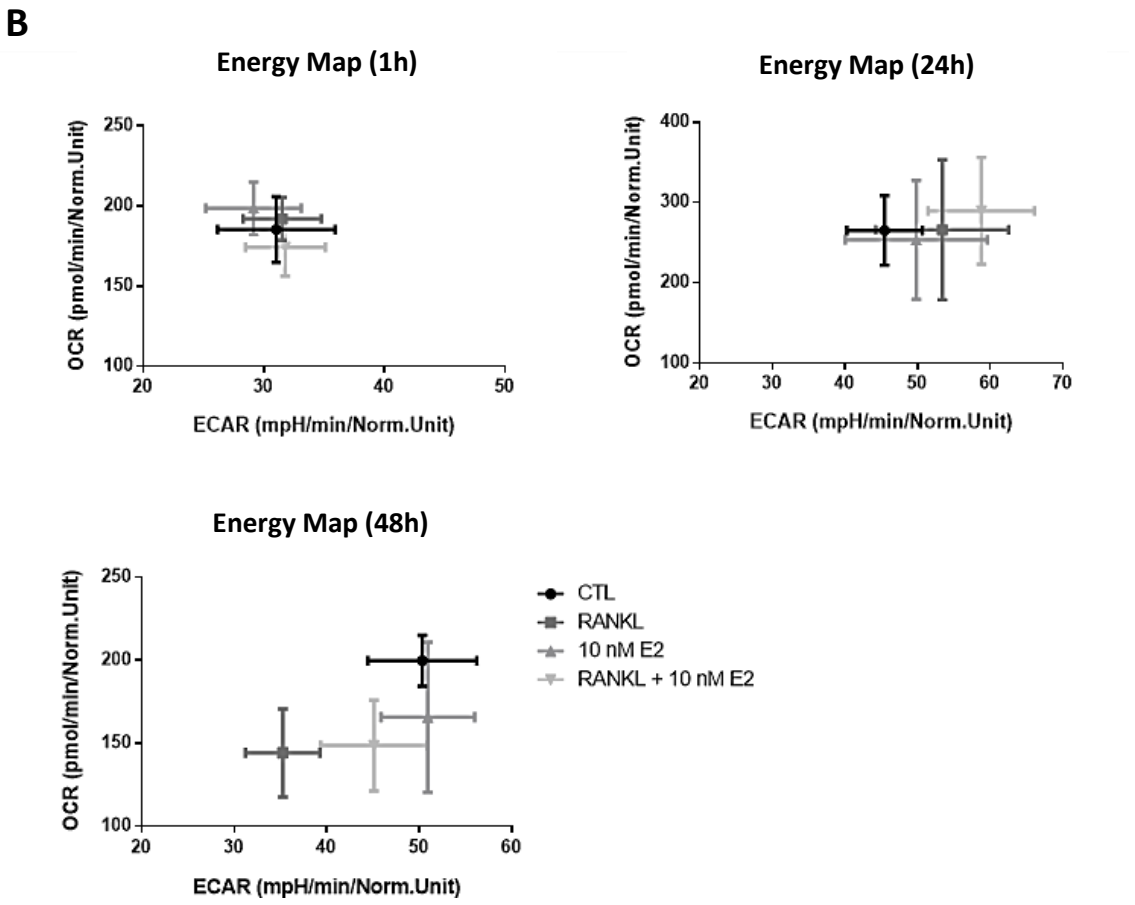

Figure 14. Mitochondrial respiratory parameters of RAW 264.7 cells exposed to 50 ng/mL of RANKL, 10 nM of E2 and 10n M of E2 plus 50 ng/mL of RANKL during 1h, 24h, and 48h, in Charcoal Stripped Medium. A) Basal respiration, maximal respiration, ATP-linked oxygen consumption rate, proton leak, non-mitochondrial respiration and spare respiratory capacity of RAW 264.7 cells exposure to 50 ng/mL of RANKL, 10 nM of E2 and 10n M of E2 plus 50 ng/mL of RANKL during 1h, 24h, and 48h. **B)** Oxygen consumption rate (OCR) versus extracellular acidification rate (ECAR) after RAW 264.7 cells exposure to 50 ng/mL of RANKL, 10 nM of E2 and 10n M of E2 plus 50 ng/mL of RANKL for 1h, 24h, and 48h. All data are presented as mean ±SEM of 4 replicates of 4 independent experiments. SRB technique was used for normalizing the obtained data.*P < 0.05 and **P < 0.01.

In general, no significant differences were observed in the obtained results with exception for proton leak-OCR (**Fig. 14A**). The incubation of RAW 264.7 macrophages with 10 nM of E2 and 50

ng/mL of RANKL for 24 hours produced an increase in oxygen consumption rate when compared to the control and with the 24 hours incubation with 10 nM of E2 alone.

Regarding the cells energetic profile, at 48 hours the results show an interesting effect of E2 which seems to produce a contrary effect of the one caused by RAW 264.7 incubation with RANKL. RAW 264.7 incubated with 10 nM of E2 for 48 hours seem to acquire a slightly more glycolytic profile which can be translated by a slight increase in ECAR, when compared to RAW 264.7 incubated with 50 ng/mL of RANKL for 48 hours (**Fig. 14B**). Moreover, the energy map graph correspondent to 24 hours of exposure showed that RAW 264.7 cells exposed to 10 nM of E2 together RANKL had an increased ECAR and OCR, presenting a more energetic profile than control and remaining treatments. The results regarding 1 hour of exposure to 50 ng/mL of RANKL, 10 nM E2 and 10 nM E2 plus RANKL, showed no clear differences in ECAR or changes in RAW 264.7 cells energetic profile.

4.4. Alterations induced by RANKL, estrogen and estrogen receptor alpha and beta antagonists in cellular ROS production of RAW 264.7 macrophages in charcoal stripped medium

In this chapter, we began to explore the effect of the antagonists of estrogen receptor alpha and beta, MPP and PHTPP respectively, in the differentiation of RAW 264.7 macrophages into osteoclasts. Therefore we incubated RAW 264.7 cells with 10 nM of MPP and 10 nM of PHTPP in the presence and absence of RANKL during 6 and 24 hours. Additionally, taking into account previous findings that suggest that estrogen is capable of attenuating oxidative stress[129], RAW 264.7 were also incubated with 10 nM of E2 in the presence and absence of RANKL for 6 and 24 hours. Culture medium containing charcoal stripped FBS was used in this assay so that estrogen usually present in FBS would not interfere with the obtained results.

RAW 264.7 exposure to 50 ng/mL of RANKL for 6 and 24 hours did not result in significant alterations in ROS production when compared to the control, although a slight increase (P= 0.0679) in ROS production can be observed after 6 hours exposure when compared to the control (**Fig. 15A**).

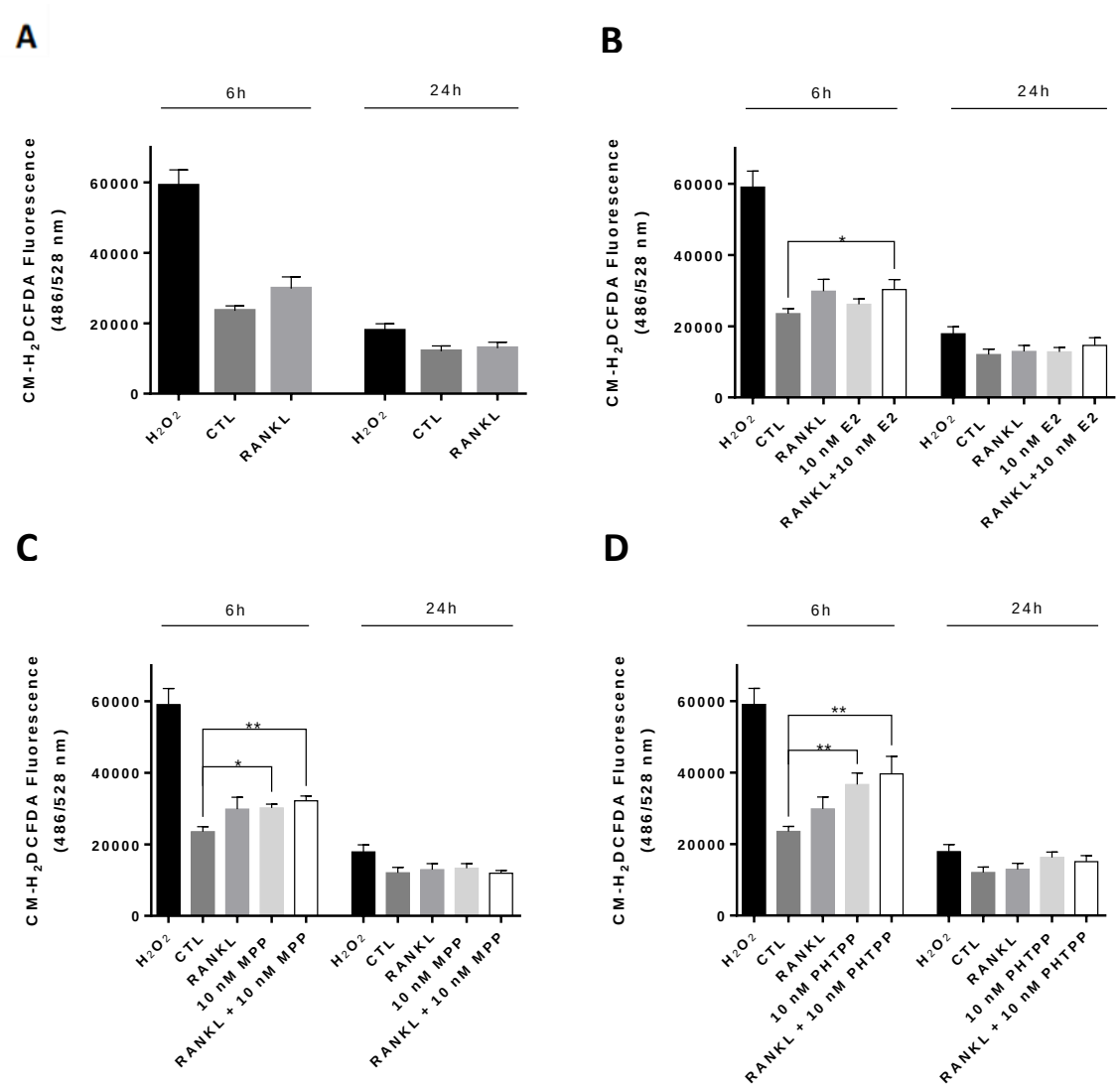

Figure 15. Cellular ROS production of RAW 264.7 macrophages exposed 6 and 24 hours to different conditions in Charcoal Stripped Medium: A) 50 ng/mL of RANKL; **B)** 50 ng/mL of RANKL, 10 nM of E2, and 10 nM of E2 plus 50 ng/mL of RANKL; **C)** 50 ng/mL of RANKL, 10 nM of MPP, and 10 nM of MPP plus 50 ng/mL of RANKL; and **D)** 50 ng/mL of RANKL, 10 nM of PHTPP, and 10 nM of PHTPP plus 50 ng/mL of RANKL. ROS measurement was performed using CM-H_2DCFDA dye and RAW 264.7 cells treated with 10 mM of H_2O_2 were used as a positive control. Data are presented as mean ±SEM of 4 replicates of 3 independent experiments. SRB technique was used as normalization procedure. *P < 0.05 and **P < 0.01.

After 6 hours of incubation with 50 ng/mL of RANKL plus 10 nM of E2, RAW 264.7 showed an increased cellular ROS production compared to the control (**Fig, 15B**). No significant differences were observed in cellular ROS production regarding the 24 hours of RAW 264.7 exposure to 10 nM of E2 and 10 nM of E2 plus 50 ng/mL of RANKL.

Regarding the effect of the estrogen receptor antagonists, when RAW 264.7 macrophages were exposed to 10 nM of MPP and 10 nM of MPP plus 50 ng/mL of RANKL for 6 hours, an increase in cellular ROS production was observed (**Fig. 15C**). The same result was not observed after 24 hours of RAW 264.7 exposure to the same treatments, where no significant differences were observed.

Finally, cells exposed to 10 nM of PHTPP and 10 nM of PHTPP plus 50 ng/mL of RANKL for 6 hours showed an increased cellular ROS production when compared to the control (**Fig. 15D**). No significant differences were observed in RAW 264.7 cells exposed to the same treatments for 24 hours.

5. DISCUSSION

RAW 264.7 macrophages are frequently used as an *in vitro* cellular model to study osteoclasts differentiation and activity since they have the ability to differentiate into mature and active osteoclasts upon exposure to RANKL[130,131]. These adherent cells possess simple and replicable culture conditions. In addition, being sensitive to RANKL, once they differentiate, RAW 264.7 acquire morphological and functional hallmark characteristics of fully differentiated osteoclasts[130]. These advantages, along with the fact that the use of a cellular line, instead of primary cells, avoid the use of animals in laboratory, RAW 264.7 cell line was the chosen biological model for the present study. Our first objective was to confirm osteoclasts differentiation from RAW 264.7 cell line and characterize the differentiated cells, in order to validate our experimental conditions. Thus, in order to achieve our goal, we cultured RAW 264.7 macrophages in high glucose (25 mM) DMEM media in the presence and absence of 50 ng/mL of RANKL for 6 days. After that time period, multinucleated and TRAP-positive cells were counted to define the percentage of differentiated osteoclasts (**Fig. 8A**). From our results, we observed that only 2.7% of the total cells were multinucleated and TRAP-positive. Since we were aware that the obtained percentage of differentiation was very low, we then tested another marker of osteoclast differentiation, the protein levels of cathepsin K. Cathepsin K is a protease released by mature osteoclasts responsible for the degradation of type I collagen during osteoclast-mediated bone resorption[124,132]. In our results, we observed that levels of cathepsin K in RAW 264.7 macrophages were already increased after 3 days of exposure to 50 ng/ml of RANKL and maintained high until day 6 of differentiation (**Fig. 8B**). Although the percentage of differentiated osteoclast, determined by the TRAP-staining method, was very low, RAW 264.7 cells increased the synthesis of cathepsin K after exposure to RANKL, indicating that those cells appear to be differentiating into mature and active osteoclasts. Furthermore, the differentiation process appears to start earlier than 3 days of exposure to RANKL, which was already observed in previous similar studies where bone marrow macrophages (BMMs) were used to obtain osteoclasts[133]. The low

percentage of obtained mature osteoclasts is possibly explained by the short lifespan of osteoclasts[134]. This would suggest that, at day 6 of RANKL exposure, some of the previously formed osteoclasts have already died, contributing to a smaller percentage of differentiated cells.

The cellular differentiation process requires alterations in the cells metabolism in order to provide them the energy they need to proliferate and differentiate[135]. These alterations occur as an adaptation and therefore, it is expected that differentiated cells show altered mitochondrial respiration or glycolysis, as a response to a different energy demand. Therefore, our next goal was to evaluate how cellular metabolism changes during RANKL-mediated osteoclast differentiation. For this, after exposure to 50 ng/mL of RANKL for 1, 3 and 6 days, a metabolic analysis using the XFe technology, initially developed by Seahorse Biosciences, was performed.

Previous studies where BMMs were used to obtain osteoclasts showed that, after differentiation, the cells exhibited an increased oxygen consumption and extracellular acidification, revealing raised oxidative phosphorylation and glycolysis levels[136,137]. Regarding the RAW 264.7 cell line, there are previous studies where RANKL-induced differentiation into osteoclasts led to an increased expression of tricarboxylic acid cycle and oxidative phosphorylation enzymes[138]. Despite these results, there seems to be no information regarding these enzymes activity during RAW 264.7 macrophages differentiation into osteoclasts. Meanwhile, our results showed that RAW 264.7 cells exposed to 50 ng/mL of RANKL during 1, 3 and 6 days presented a significant decrease in OCR associated with basal respiration, maximal respiration, ATP-linked respiration as well as proton leak (**Fig. 9A**). In addition, the obtained results suggest a diminished OCR and ECAR, revealing a more quiescent cellular profile upon RAW 264.7 macrophages exposure to RANKL, which was accentuated from day 1 to day 3 reaching the lowest levels at day 6 (**Fig. 9A, B**). Taken together, our results seem to contradict what is described in the existing literature. Relatively to the studies performed in BMMs, the different outcome in our results may be explained by the different choice of the biological model. Different origins of BMM and RAW 264.7 have a distinct influence on cell

behavior and the two cell types may present different basal metabolism[139]. Our hypothesis to explain the obtained results is that the decrease in OCR and ECAR, which can be translated in a decrease in oxidative phosphorylation and glycolysis, respectively, may be associated with the fact that the RAW 264.7 cells are becoming less proliferative along differentiation and committing to the osteoclastic lineage. This would imply that, as the differentiation process advances, the cells would require less energy to proliferate, becoming, as observed, more quiescent. Another hypothesis to explain our results is the possibility of a mitochondrial dysfunction occurrence, increased along the RANKL exposition period. In this case scenario, RANKL would act as a stress inducer which could cause mitochondrial dysfunction suggested by the diminished OCR and ATP-linked respiration depletion. Although, this theory does not explain the decreased ECAR along RAW 264.7 differentiation. Since the cells have a lower reliance on oxidative phosphorylation, the glycolytic path should be increased for ATP production. In this case, increased glycolysis would lead to an increased ECAR due to the reduction potential regeneration trough lactate production. This second hypothesis to explain the obtained results was formed taking into account the increased expression of TCA and oxidative phosphorylation enzymes observed in the previously mentioned papers[136,137]. We rely on the hypothesis that if there is an increased protein expression along RAW 264.7 differentiation, but once the same pattern is not observed in OCR and ATP- linked respiration, there could be a mitochondrial dysfunction.

Mitochondrial dysfunction can be characterized by a reduced ATP production by oxidative phosphorylation, inability to modulate ROS production, dysregulation of calcium and even apoptosis[140]. There is a large multitude of causes that can lead to mitochondrial dysfunction being the most common associated with mtDNA mutations leading to defects, for example, on subunits of the OXPHOS machinery that are encoded by mtDNA[141]. Therefore, and to better understand the previously obtained results, our next goal was to evaluate the protein levels of Complex I, Complex II, Complex III, Complex IV and ATP synthase of the mitochondrial electron transport chain in RAW

264.7 cells exposed to 50 ng/mL of RANKL for 3 days and 6 days. To each complex and ATP synthase, specific subunit antibodies were tested. The tested subunits were NDUFB8, SDHB, UQCRC2, and ATP5A, from Complex I, Complex II, Complex III, and ATP synthase, respectively, encoded by nuclear DNA, and subunit MTCO1, from Complex IV, encoded by mitochondrial DNA. Although our results regarding the protein expression levels presented no significant differences, it is possible to observe an apparent increase in the protein levels of Complex II, Complex III, Complex IV in cells exposed to RANKL when compared to RAW 264.7 control cells (**Fig. 10**). These results, together with the results regarding the ratio of mtDNA/ nDNA copy number could suggest increased mitochondrial biogenesis during RAW 264.7 macrophages differentiation into osteoclasts. Although not statistically significant, probably due to the low number of values for statistical analysis, the results suggested an increase in mtDNA copy number after RAW 264.7 exposure to 50 ng/mL of RANKL for 3 and 6 days (**Fig. 11**). This outcome is in agreement with several lines of evidence that show that mitochondrial biogenesis is augmented during osteoclast differentiation[142]. In addition, osteoclasts are described as cells rich in mitochondria, which would explain high levels of mtDNA copy number[143]. Although these lines of evidence do not imply an increased mitochondrial function along with osteoclasts differentiation. Therefore, another possible explanation for this result is that increased mitochondrial biogenesis may be occurring as a cellular attempt to overcome a mitochondrial dysfunction acting as a defense mechanism. To better understand what is happening during RAW 264.7 macrophages differentiation into osteoclasts it would be interesting to analyze specifically the expression levels of mitochondrial complexes and ATP synthase activities as well as complexes subunits and assembly factors.

ROS production is an important characteristic of osteoclastogenesis since ROS act as second messengers in signaling pathways involved in the differentiation process, including NFκB, MAPK, and Ca^{2+}-mediated signaling, being also important for osteoclasts resorption activity[144,145]. Although, an increased ROS production can also be the consequence of an impaired mitochondrial

function[146]. Taking this into account, our next step was to evaluate RAW 264.7 macrophages cellular and mitochondrial ROS production after 6 days of exposure to 50 ng/mL of RANKL. In order to do so, CM-H_2DCFDA and MitoSOX fluorescent probes were used to measure cellular and mitochondrial ROS, respectively. Our results show a significant increase both in cellular and mitochondrial ROS production after RAW 264.7 exposure to RANKL when compared to the RAW 264.7 control cells (**Fig. 12A, B**). This outcome is in agreement with the previously mentioned literature where ROS are presented as key second messengers to RANKL-mediated osteoclast differentiation. Although, regarding our previous theory that RANKL exposure may cause mitochondrial dysfunction along the differentiation process, the increased ROS production may also be a signal of mitochondrial function impairment. In this case scenario, ROS accumulation along time can be involved in the induction of osteoclasts apoptosis as a result of oxidative stress[147]. Taking this into account, alterations in RAW 264.7 mitophagy and apoptosis after exposure to RANKL would be good parameters to be evaluated in the future, considering that little is known about osteoclast apoptotic and mitophagic mechanisms.

Moreover, focusing on mitochondrial ROS production, studies performed in BMM showed that, during differentiation, SOD2 expression can be increased by RANKL action[58]. This enzyme constitutes a mitochondrial antioxidant defense that catalyzes the dismutation of superoxide radicals to hydrogen peroxide[148]. Taken this into account, and the fact that RAW 264.7 cells presented an augmented ROS production after 6 days of exposure to RANKL, we thought it could be interesting to analyze what was happening to SOD2 during RAW 264.6 macrophages differentiation. Therefore, we preceded to evaluate this enzyme expression levels by Western Blot after RAW 264.7 exposure to 50 ng/mL of RANKL for 3 and 6 days. In our results, as expected according to the existing literature, there seems to be a slight increase in SOD2 expression at day 6 of RANKL exposure, although the differences were not statistically significant (**Fig. 12C**). This increase may be a consequence of an increased ROS production at day 6 of RANKL exposure. In this way, SOD2 levels

would increase as an attempt to lower mitochondrial ROS levels and prevent oxidative damage. On another hand, since it is described that RANKL upregulates SOD2 expression, in our results we may only be observing a mechanism of negative feedback to prevent the formation of an excessive number of osteoclasts by the decreasing of ROS levels. In this matter, more studies would have to be performed to assess ROS formation during RAW 264.7 differentiation to deny or confirm the correlation between ROS levels and mitochondrial dysfunction and the relation with SOD2 expression.

There are several lines of evidence showing that E2 can play a protective role against ROS in several body tissues[48]. Since ROS play an important role in RANKL-mediated osteoclasts differentiation, E2 effect, attenuating ROS levels will impair NF-kB activation, therefore decreasing osteoclastogenesis[45,149]. Taking these findings into consideration, our next goal was to understand how RAW 264.7 cellular metabolism can change when E2 is added to the equation. As we did not know what was the immediate effect of RANKL neither E2 on RAW 264.7 macrophages, first, we performed an assay to test the acute effect of these compounds on RAW 264.7 metabolic profile. In order to do so, we exposed RAW 264.7 cells to 50 ng/mL of RANKL, 100 nM of E2 and 1 μM of E2, individually, and used the XFe technology developed by Seahorse Bioscience to assess OCR-related changes. Our results demonstrated that in response to an acute injection of 50 ng/mL of RANKL there was a significant increase in RAW 264.7 macrophages OCR. No significant differences were observed regarding both concentrations of E2, although OCR seems to be increased when compared to RAW 264.7 control cells (**Fig. 13**). To explain this results, our main hypothesis was that, when RAW 264.7 macrophages are first exposed to RANKL they may need a high energy input to start the differentiation process, which becomes less significant as they become mature osteoclasts, which is in agreement with the previously obtained results shown in **Figure 9**. Therefore, the uncoupling of the electron transport chain and ATP synthase may be occurring in the precise moment of the RANKL injection, due to a great increase in ROS production. This would explain why

the same increase is not observed in the parameter regarding ATP-linked respiration. Regarding E2, although RAW 264.7 macrophages increased OCR in acute response is not statistically significant, there is a significant increase both in ATP-linked respiration and Proton Leak regarding both tested concentrations (**Fig. 13**). Acknowledging that E2 impairs osteoclastogenesis, contrarily to RANKL, which promotes differentiation, we initially thought that we would observe opposite effects on RAW 264.7 macrophages metabolism regarding the two compounds. Although our outcome was not quite what we first speculated, a previous study using 1 μM of Genistein, a compound that mimics 17β-estradiol, showed that it promotes mitochondrial respiration through AMP-activated protein kinase (AMPK) activation in RAW 264.7 macrophages after 18 hours of exposure[150]. The AMPK activation suppresses NF-kB signaling and ROS signaling, promoting E2 protective effect against oxidative damage[151]. Therefore, regarding the estradiol effect on RAW 264.7 macrophages metabolism, our results are in agreement with the existing literature. Although, it is necessary to better understand E2 impact during RANKL- mediated osteoclast differentiation, along with its impact on RAW 264.7 cellular metabolism after longer exposition periods. Thus, we exposed RAW 264.7 cells to 50 ng/mL of RANKL, 10 nM of E2 and 50 ng/mL of RANKL plus 10 nM of E2 for 1h, 24h and 48h and then performed a metabolic analysis using XFe technology developed by Seahorse. At this point, taking into account our previous results where RAW 264.7 differentiation into osteoclasts seemed to start earlier than day 3 or RANKL exposure, we decided to use shorter time points as an attempt to understand what was happening to RAW 264.7 OCR and ECAR and earlier stages of the differentiation process. In this experiment we also used a lower concentration of E2 as an attempt to see if its impact on RAW 264.7 macrophages would be similar to the previously obtained result. 10 nM was the chosen concentration, as it was described to resemble more 17β-estradiol physiological conditions[152]. In addition, in this assay, culture medium supplemented with charcoal stripped FBS was used to avoid that estrogens, normally present in FBS, would interfere with the obtained results. Using this culture medium, it is important to be aware that the FBS treatment with dextran-coated charcoal removes not only estrogen, but also steroids, growth factors, lipids and other hormones[110].

In our results, we observed that RAW 264.7 exposure to combined RANKL and E2 for 24h resulted in a significant increase in OCR-linked proton leak when compared to RAW 264.7 control cells and RAW 264.7 exposed to 10 nM of E2 only (**Fig. 14A**). Although no other significant differences were obtained, it is possible to observe that, in general, it seems that at 24h there are more differences regarding RAW 264.7 OCR between the different treatments. In fact, there seems to be a slight decrease in basal respiration, maximal respiration and ATP-linked respiration in presence of 50 ng/mL of RANKL accompanied by a decrease in OCR-linked proton leak. This is in agreement with our previous theory that RANKL can induce some kind of stress to the cell causing mitochondrial dysfunction. Still relatively to 24h of exposition, regarding E2, RAW 264.7 seem to show a decrease in basal, maximal, ATP-linked and proton leak associated respiration when compared to control cells. In this way, estradiol alone, seemed to produce in RAW 264.7 macrophages a similar effect to the one caused by RANKL. Although, when cells were incubated with both RANKL and E2 for 24h, their OCR seemed to increase to an even higher level than control cells. Since E2 impairs ROS production and osteoclast differentiation, we expected that, when in presence of RANKL, E2 would act in order to contradict its effect on RAW 264.7 cells, therefore increasing their metabolic activity. We expected that, in presence of both compounds, OCR would be at a level similar to the one in control cells. Although the observed increase was higher, the outcome is in agreement with our expectations. At 48h of exposure, all OCR related parameters seem to be lower, which could be an indicator characteristic pattern of a more advanced state of RAW 264.7 differentiation, as it was observed in previous results (**Fig. 9**). Although, we cannot take firmer conclusions regarding different exposition periods, as these groups were not compared amongst each other. Regarding 1h of RAW 264.7 exposure, all measured OCR-related parameters seemed to present little variations between the treatment groups, which was confirmed by the obtained energy map (**Fig. 14B**). This observation may be an indicator that 1h of exposure may not be a good time point to changes regarding RAW 264.7 cellular metabolism. Regarding RAW 264.7 cells energetic profile, the energy map correspondent to 24h of exposure showed that RAW 264.7 cells exposed to E2 together RANKL had an increased

ECAR and OCR, presenting a more energetic profile than control and remaining treatments. Once again, this outcome agrees what we first expected. Since RANKL induce in RAW 264.7 a more quiescent profile, it would be expected that E2 would counteract this tendency, producing an increase in both glycolysis (ECAR) and oxidative phosphorylation (OCR). Moreover, at 48 hours the results show that E2 which seems to produce a contrary effect in RAW 264.7 of the one caused by RANKL incubation. Here, there seems to be an increase in the ECAR of RAW 264.7 macrophages exposed to E2, which can be translated as a more glycolytic profile, closer to the one observed in control cells (**Fig. 14B**). In a general, our results seem to demonstrate that estradiol stimulates RAW 264.7 glycolysis. This effect has already been observed in other studies where estrogen receptor-positive breast cancer cells exposed to E2 developed a more glycolytic profile[153].

Taking into account our previous results, that confirmed E2 impact on RAW 264.7 macrophages differentiation into osteoclasts, our next goal was to try to understand the mechanisms behind its action. ERα and ERβ are the most abundant type of estrogen receptors in the organism, and they are already known to exist in multiple bone cell types, being one of them osteoclasts[83]. Therefore, as an attempt to understand which receptor had a more significant role mediating osteoclast differentiation, we used synthetic specific antagonists for each one of them: MPP for ERα, and PHTPP for ERβ[104]. In this first approach, we only began to explore the effect of MPP and PHTPP alone RAW 264.7 macrophages cellular ROS production. In order to do so, RAW 264.7 cells were incubated with 10 nM of E2, 10 nM of MPP and 10 nM of PHTPP in the presence and absence of 50 ng/mL of RANKL during 6 and 24 hours, and cellular ROS production was assessed using CM-H_2DCFDA fluorescent probe. In this assay, once again, charcoal stripped FBS was used to avoid that estrogens present in the culture medium would interfere. Regarding RANKL alone, although slightly increased, no significant differences were observed in RAW 264.7 ROS production in both time points (**Fig. 15A**). Taking into account our previous results where RAW 264.7 cellular ROS production increased significantly after 6 days of exposure to RANKL (**Fig. 12A**), in this case scenario, the shorter RANKL

incubation periods may have not been enough to observe any significant differences. Therefore, further experiments with intermediate periods of RANKL exposure should be performed to assess RAW 264.7 ROS production during differentiation. Regarding E2, after 6 hours of incubation together with RANKL, RAW 264.7 macrophages had an increased cellular ROS production when compared to the control (**Fig, 15B**). Since E2 is known to attenuate ROS levels, we first expected that RAW 264.7 cells exposed both to E2 and RANKL would have a ROS production similar to the control. As we did not observe this outcome, maybe the concentration of E2 that we tested was not enough to impair ROS signaling and osteoclast differentiation. Instead, E2 and RANKL seemed to produce a synergetic effect when added together to RAW 264.7 macrophages. Furthermore, our results regarding ER antagonists showed that RAW 264.7 cells exposed to MPP and MPP plus RANKL for 6 hours had an increased cellular ROS production when compared to the control cells (**Fig. 15C**). The same result was observed regarding PHTPP (**Fig. 15D**). Regarding these results, our hypothesis is that FBS treatment with dextran-coated charcoal may not have completely removed all estrogen. This would explain why RAW 264.7 macrophages exposed to antagonists alone have a higher level of cellular ROS production when compared to the control cells. As MPP and PHTPP antagonize ERα and ERβ, respectively, estrogen action is impaired, increasing ROS levels. In control, without the antagonists, some of the estrogen remaining in the culture medium may have impaired ROS production, contributing to lower ROS levels. Furthermore, the present results suggest that, in general, RAW 264.7 differences in cellular ROS production are more significant at 6h of treatment exposure, presenting higher ROS levels. Taking into account that the same pattern is observed in positive controls and control cells, our hypothesis is that the RAW 264.7 cells culture in charcoal-stripped medium for a larger period of time may somehow modulate their ROS production. Overall, regarding this topic, our results demonstrated that ERβ antagonization causes a higher level of cellular ROS production than ERα antagonization, suggesting that ERβ may have a determinant role regarding E2 signaling in RAW 264.7 macrophages. Although, being only a preliminary experiment to discover

which ER has a more significant role mediating estradiol effect on osteoclast differentiation, this study is not complete, and no firmer conclusions can be drawn.

CONCLUSIONS

In this study, we successfully differentiated RAW 264.7 macrophages into osteoclasts upon RANKL exposure. After 6 days of exposure, the obtained cells expressed cathepsin K and TRAP, hallmark of active and mature osteoclasts, therefore validating RAW 264.7 as a good *in vitro* model to study osteoclast differentiation. Furthermore, our data suggest that the differentiation process may begin earlier than it is suggested by the literature, as cathepsin K levels are already increased at day 3 of RANKL exposure.

Regarding RAW 264.7 macrophages cellular metabolism, we demonstrated that, RANKL exposure negatively influences mitochondrial performance, inducing a more quiescent metabolic profile. In addition, our results also show that, after 6 days of RANKL exposure, cellular and mitochondrial ROS production are greatly increased in RAW 264.7. Therefore, we propose that mitochondrial dysfunction, as a consequence of a long term RANKL exposure, may have a significant impact on bone turnover and it may be an influencing factor to osteoporosis appearance.

Regarding the effect of E2 on RAW 264.7 macrophages differentiation into osteoclasts, the obtained results were not robust enough to draw a solid conclusion and it would be necessary to perform more experiments in order to do so.

However, overall, our results obtained allowed us to observe that mitochondria plays a relevant role in the osteoclast differentiation process, and may be a potential target for the development of new therapeutic strategies for osteoporosis.

FUTURE EXPERIMENTS

The present study contains several limitations that should be overcome in future experiments in order to continue exploring possible targets that may allow the development of new therapeutic strategies for osteoporosis. Thus, we identified three main points to be improved:

1) Some of the experiments described in this study, principally regarding Western Blot and qRT-PCR, present an absence of significant differences that may be due to a low number of independent experiments. Therefore, in the future, it would be necessary to increase the number of independent experiments to a minimum of n=4 or n=5 in every experiment.

2) Taking into account some of our results, it is possible that charcoal stripped FBS may still contain a residual estrogen amount. Before future experiments, it would be important to quantify the estrogen concentration both in normal FBS and charcoal stripped FBS, in order to validate or deny this possibility.

3) Although RAW 264.7 macrophages are described as a good *in vitro* model to study osteoclastogenesis, it would be important to perform our study in parallel with primary cells or another cell line, in order to compare results and corroborate or not some of our formulated hypothesis.

Furthermore, in order to complete our study and answer some of the questions that were raised by the obtained results, we purpose a few future experiments. Taking into account that it was not possible to precisely determine the time that follows since RANKL addition until the formation of mature osteoclasts, in the future it would be interesting to assess the expression of mature osteoclast markers also at earlier time points, for example day 1 and day 2 of RANKL exposition. Mitochondrial ROS production should also be assessed at shorter time periods after RANKL exposure, for example 6h and 24h as it was performed for cellular ROS. Additionally, we think it would be interesting to

assess cellular and mitochondrial ROS production at day 2 and day 3 of RAW 264.7 differentiation, therefore allowing to have a better notion of what is happening to ROS production during several differentiation stages. In this parameter, we could also assess Sirtuin 3 protein levels and compare it with SOD2 levels (with an increased number of independent experiments). Sirtuin 3 deacetylates SOD2 lysine residues therefore activating it and consequently reducing ROS levels. Therefore, during osteoclastogenesis, if there are variations in SOD2 levels, it would make sense that they should also be observed in Sirt3. Moreover, to further understand our results regarding RAW 264.7 mitochondrial respiratory parameters alterations in presence of 50 ng/mL RANKL and 10 nM of E2, in the same conditions we should assess RAW 264.7 glycolytic rate, mitochondrial network, mitochondrial morphology and mitochondrial membrane potential. Regarding the use of MPP and PHTPP, it the future, it would be important to assess their impact not only on cellular ROS production, but also mitochondrial ROS production both in presence of RANKL and E2 as well. Finally, it would also be interesting to analyze the impact that these antagonists can have in mitochondrial respiration and glycolytic rate during RAW 264.7 macrophages differentiation, both in presence and absence of E2.

References

1. White, T. D. and F. P. A. *The Human Bone Manual*. (2005).

2. Clarke, B. Normal bone anatomy and physiology. *Clin. J. Am. Soc. Nephrol.* **3 Suppl 3,** 131–139 (2008).

3. Florencio-silva, R. *et al.* Biology of Bone Tissue : Structure , Function , and Factors That Influence Bone Cells. **2015,** (2015).

4. Langdahl, B., Ferrari, S. & Dempster, D. W. Bone modeling and remodeling: potential as therapeutic targets for the treatment of osteoporosis. *Ther. Adv. Musculoskelet. Dis.* **8,** 225–235 (2016).

5. Fakhry, M., Hamade, E., Badran, B., Buchet, R. & Magne, D. Molecular mechanisms of mesenchymal stem cell differentiation towards osteoblasts. **5,** 136–148 (2013).

6. Lieben, L., Callewaert, F. & Bouillon, R. Bone and metabolism: A complex crosstalk. *Horm. Res.* **71,** 134–138 (2009).

7. Capulli, M., Paone, R. & Rucci, N. Osteoblast and osteocyte: Games without frontiers. *Arch. Biochem. Biophys.* **561,** 3–12 (2014).

8. Xiong, J. *et al.* Osteocytes, not osteoblasts or lining cells, are the main source of the RANKL required for osteoclast formation in remodeling bone. *PLoS One* **10,** 1–19 (2015).

9. Mason, A. Osteoclasts: more than 'bone eaters'. **19,** 389–399 (2009).

10. Brien, C. A. O. Control of RANKL Gene Expression. **46,** 911–919 (2011).

11. Matic, I. *et al.* Quiescent Bone Lining Cells Are a Major Source of Osteoblasts During Adulthood. *Stem Cells* **34,** 2930–2942 (2016).

12. Kristensen, H. B., Andersen, T. L., Marcussen, N., Rolighed, L. & Delaisse, J. M. Osteoblast recruitment routes in human cancellous bone remodeling. *Am. J. Pathol.* **184,** 778–789 (2014).

13. Xing, L., Schwarz, E. M. & Boyce, B. F. Osteoclast precursors, RANKL/RANK, and immunology. *Immunol. Rev.* **208,** 19–29 (2005).

14. Zhao, Q., Shao, J. & , Wei Chen, Y.-P. L. Osteoclast differentiation and gene regulation. 2519–2529 (2007).

15. Kubatzky, K. F., Uhle, F. & Eigenbrod, T. From macrophage to osteoclast – How metabolism determines function and activity. *Cytokine* 0–1 (2018). doi:10.1016/j.cyto.2018.06.013

16. Lee, K. *et al.* Selective Regulation of MAPK Signaling Mediates RANKL-dependent Osteoclast Differentiation. **12,** (2016).

17. Soysa, N. S., Alles, N., Aoki, K. & Ohya, K. Osteoclast formation and differentiation: An overview. *J. Med. Dent. Sci.* **59,** 65–74 (2012).

18. Coughlan, T. & Dockery, F. Osteoporosis and fracture risk in older people. *Clin. Med. (Northfield. Il).* **14,** 187–191 (2014).

19. Kanis, J. A. *et al.* Ten year probabilities of osteoporotic fractures according to BMD and diagnostic thresholds. *Osteoporos. Int.* **12,** 989–995 (2001).

20. Kanis, J. A. *et al.* A family history of fracture and fracture risk: a meta-analysis. *Bone* **35,** 1029–37 (2004).

21. Kanis, J. A. *et al.* Alcohol intake as a risk factor for fracture. *Osteoporos. Int.* **16,** 737–742 (2005).

22. Kanis, J. A. *et al.* Smoking and fracture risk: A meta-analysis. *Osteoporos. Int.* **16,** 155–162 (2005).

23. Namba, S. *et al.* Long-term warfarin therapy and biomarkers for osteoporosis and atherosclerosis. *BBA Clin.* **4,** 76–80 (2015).

24. Rinaldi, R. Z. Aromatase Inhibitor Adjuvant Chemotherapy of Breast Cancer Results in Cancer Therapy Induced Bone Loss. *Curr. Osteoporos. Rep.* **11,** 61–64 (2013).

25. Fernie, A. R., Carrari, F. & Sweetlove, L. J. Respiratory metabolism : glycolysis , the TCA cycle and mitochondrial electron transport. 254–261 (2004). doi:10.1016/j.pbi.2004.03.007

26. Mookerjee, S. A., Gerencser, A. A., Nicholls, D. G. & Brand, M. D. Quantifying intracellular rates of glycolytic and oxidative ATP production and consumption using extracellular flux. **292,** 7189–7207 (2017).

27. Herzig, Sébastien;Raemy, Etienne; Montessuit, Sylvie; Veuthey, Jean-Luc; Zamboni, Nicola; Westermann, Benedikt; Kunji, Edmund R. S. and Martinou, J.-C. Identification and Functional Expression of the Mitochondrial Pyruvate Carrier. *Science (80-.).* **93,** (2012).

28. Shi, L. & Tu, B. P. Acetyl-CoA and the Regulation of Metabolism: Mechanisms and

Consequences. *Curr Opin Cell Biol* 125–131 (2016). doi:10.1016/j.ceb.2015.02.003.Acetyl-CoA

29. Akram, M. & Szent-gyo, A. Citric Acid Cycle and Role of its Intermediates in Metabolism. *Cell Biochem Biophys* 475–478 (2014). doi:10.1007/s12013-013-9750-1

30. Osellame, L. D. *et al.* Cellular and molecular mechanisms of mitochondrial function. *Best Pract. Res. Clin. Endocrinol. Metab.* **26,** 711–723 (2012).

31. Nicholls, David G and Ferguson, S. J. *Bioenergetics 3*. (2001).

32. Rich, P. R. & Maréchal, A. The mitochondrial respiratory chain. 1–23 (2010). doi:10.1042/BSE0470001

33. Sousa, J. S., Imprima, E. D. & Vonck, J. *Mitochondrial Respiratory Chain Complexes*. (2018).

34. Valvona, C. J., Fillmore, H. L., Nunn, P. B. & Pilkington, G. J. The Regulation and Function of Lactate Dehydrogenase A : Therapeutic Potential in Brain Tumor. *Brain Pathol.* (2015). doi:10.1111/bpa.12299

35. Pineda, J. R. E. T., Callender, R. & Schwartz, S. D. Ligand Binding and Protein Dynamics in Lactate Dehydrogenase. *Biophys. J.* **93,** 1474–1483 (2007).

36. Warburg, O. & Wind, F. The Metabolism of Tumors in the Body. (1926).

37. Indo, H. P. *et al.* Role of Mitochondrial Reactive Oxygen Species in the Activation of Cellular Signals , Molecules , and Function. (2017). doi:10.1007/164

38. Kehrer, J P; Tipple, T E; Robertson, J. D. and S. C. V. *Free Radicals and Reactive Oxygen Species*. *Reference Module in Biomedical Research* (Elsevier Inc., 2015). doi:10.1016/B978-0-12-801238-3.01895-X

39. Phaniendra, A. & Babu, D. Free Radicals : Properties , Sources , Targets , and Their Implication in Various Diseases. **30,** 11–26 (2015).

40. Turrens, J. F. Mitochondrial formation of reactive oxygen species. *J. Physiol.* **2,** 335–344 (2003).

41. Wu, X. Z. Z., Wei, Y. & Yu, J. D. G. Induction of autophagy by salidroside through the AMPK-mTOR pathway protects vascular endothelial cells from oxidative stress-induced apoptosis. *Mol. Cell. Biochem.* (2016). doi:10.1007/s11010-016-2868-x

42. Zou, X. *et al.* Manganese superoxide dismutase (SOD2): is there a center in the universe of mitochondrial redox signaling ? (2017). doi:10.1007/s10863-017-9718-8

43. Wu, Yu-Ting; Wu, Shi-Bei and Wei, Y.-H. Roles of Sirtuins in the Regulation of Antioxidant Defense and Bioenergetic Function of Mitochondria under Oxidative Stress. (2014). doi:10.3109/10715762.2014.920956

44. Szewczyk, A. & Wojtczak, L. Mitochondria as a Pharmacological Target. *Pharmacol. Rev.* **54,** 101–127 (2002).

45. Srivastava, S. *et al.* Estrogen Decreases Osteoclast Formation by Down-regulating Receptor Activator of NF-κB Ligand (RANKL)-induced JNK Activation. *J. Biol. Chem.* **276,** 8836–8840 (2001).

46. Chen, F., Ouyang, Y., Ye, T., Ni, B. & Chen, A. Estrogen inhibits RANKL-induced osteoclastic differentiation by increasing the expression of TRPV5 channel. *J. Cell. Biochem.* **115,** 651–658 (2014).

47. Faienza, M. F., Ventura, A., Marzano, F. & Cavallo, L. Postmenopausal osteoporosis: The role of immune system cells. *Clin. Dev. Immunol.* **2013,** (2013).

48. Almeida, M. *et al.* J BMR Estrogens Attenuate Oxidative Stress and the Differentiation and Apoptosis of Osteoblasts by DNA-Binding-Independent Actions of the ER a. **25,** 769–781 (2010).

49. Borrás, C., Gambini, J., López-Grueso, R., Pallardó, F. V. & Viña, J. Direct antioxidant and protective effect of estradiol on isolated mitochondria. *Biochim. Biophys. Acta - Mol. Basis Dis.* **1802,** 205–211 (2010).

50. Lane, R. K., Hilsabeck, T. & Rea, S. L. Biochimica et Biophysica Acta The role of mitochondrial dysfunction in age-related diseases. *BBA - Bioenerg.* **1847,** 1387–1400 (2015).

51. Pereira, C. *et al.* Investigating Drug-induced Mitochondrial Toxicity: A Biosensor to Increase Drug Safety? *Curr. Drug Saf.* **4,** 34–54 (2009).

52. Srinivasan, S. *et al.* Role of Mitochondrial Reactive Oxygen Species in Osteoclast Differentiation. **1192,** 245–252 (2010).

53. Lean, J. M., Jagger, C. J., Kirstein, B., Fuller, K. & Chambers, T. J. Hydrogen Peroxide Is Essential for Estrogen-Deficiency Bone Loss and Osteoclast Formation. **146,** 728–735 (2015).

54. Bartell, S. M. *et al.* FoxO proteins restrain osteoclastogenesis and bone resorption by attenuating H2O2accumulation. *Nat. Commun.* **5,** (2014).

55. Ambrogini, E. *et al.* Article FoxO-Mediated Defense against Oxidative Stress in Osteoblasts Is Indispensable for Skeletal Homeostasis in Mice. *Cell Metab.* **11,** 136–146 (2010).

56. Kanzaki, H., Shinohara, F., Kanako, I. & Yamaguchi, Y. Redox Biology Molecular regulatory mechanisms of osteoclastogenesis through cytoprotective enzymes. *Redox Biol.* **8,** 186–191 (2016).

57. Kim, H. *et al.* Sirtuin1 suppresses osteoclastogenesis by. 1–12 (2015). doi:10.1210/me.2015-1133

58. Kim, H. K. Y. deok L. H. J. K. Z. H. L. and H.-H. SOD2 and Sirt3 Control Osteoclastogenesis byRegulating Mitochondrial ROS. *J Bone Min. Res* (2016). doi:10.1002/jbmr.2974

59. Huh, J. *et al.* Sirtuin 3 (SIRT3) maintains bone homeostasis by regulating AMPK- PGC-1 β axis in mice. *Nat. Publ. Gr.* **3,** 1–10 (2016).

60. Kanis, J. A. Diagnosis of osteoporosis and assessment of fracture risk. *Lancet (London, England)* **359,** 1929–36 (2002).

61. Hernlund, E. *et al.* Osteoporosis in the European Union: Medical management, epidemiology and economic burden: A report prepared in collaboration with the International Osteoporosis Foundation (IOF) and the European Federation of Pharmaceutical Industry Associations (EFPIA). *Arch. Osteoporos.* **8,** (2013).

62. Melton LJ III, Atkinson EJ, O'Connor MK, et al. Bone density and fracture risk in men. *J. bone Miner. Res.* **13,** 1915–1923 (1998).

63. Kanis, J. A. *et al.* Long-term risk of osteoporotic fracture in Malmo. *Osteoporos. Int.* **11,** 669–674 (2000).

64. Johnell, O. & Kanis, J. A. An estimate of the worldwide prevalence and disability associated with osteoporotic fractures. *Osteoporos. Int.* **17,** 1726–1733 (2006).

65. Cauley, J. A. *et al.* Effects of Estrogen Plus Progestin on Risk of Fracture and Bone Mineral Density. **290,** 1729–1738 (2003).

66. Bowring, C. E. & Francis, R. M. National Osteoporosis Society ' s Position Statement on hormone replacement therapy in the prevention and treatment of osteoporosis. 63–65 (2011).

67. Hampson, S. I. I. F. G. Treatment of post-menopausal osteoporosis : beyond bisphosphonates. 13–29 (2015). doi:10.1007/s40618-014-0152-z

68. Odvina, C. V *et al.* Severely Suppressed Bone Turnover : A Potential Complication of Alendronate Therapy. **90,** 1294–1301 (2018).

69. Siris, E. S. *et al.* Denosumab for Prevention of Fractures in Postmenopausal Women with Osteoporosis. (2009).

70. Delmas, P. D. *et al.* Efficacy of Raloxifene on Vertebral Fracture Risk Reduction in Postmenopausal Women with Osteoporosis : Four-Year Results from a Randomized Clinical Trial. **87,** 3609–3617 (2018).

71. Study, A. *et al.* Effects of Bazedoxifene on BMD and Bone Turnover inPostmenopausal Women: 2-Yr Results of a Randomized,Double-Blind, Placebo-, and Active-Controlled Study. doi:10.1359/JBMR.071206

72. Iii, C. H. C., Azria, M. & Silverman, S. Salmon calcitonin : a review of current and future therapeutic indications. 479–491 (2008). doi:10.1007/s00198-007-0490-1

73. Ortolani, S. *et al.* The Effects of Strontium Ranelate on the Risk of Vertebral Fracture in Women with Postmenopausal Osteoporosis. 459–468 (2004).

74. Zanchetta, J. R. *et al.* Effects of Teriparatide [Recombinant Human Parathyroid Hormone (1-34)] on Cortical Bone in Postmenopausal Women With Osteoporosis JR.

75. Lavelle, W., Carl, A., Lavelle, E. D. & Khaleel, M. A. Vertebroplasty and Kyphoplasty. **25,** 913–928 (2007).

76. Mauvais-jarvis, F., Clegg, D. J. & Hevener, A. L. The Role of Estrogens in Control of Energy Balance and Glucose Homeostasis. **34,** 309–338 (2013).

77. Jia, M. & Gustafsson, J.-åke. Estrogen receptor alpha and beta in health and disease. **29,** 557–568 (2015).

78. Razandi, M. *et al.* Identification of a Structural Determinant Necessary for the Localization and Function of Estrogen Receptor ⎵ at the Plasma Membrane. **23,** 1633–1646 (2003).

79. Razandi, M. *et al.* Cell Membrane and Nuclear Estrogen Receptors (ERs) Originate from a Single Transcript : Studies of ER ⎵ and ER ᴺᴸ Expressed in Chinese Hamster Ovary Cells.

307–319

80. Falahati-nini, A. *et al.* Relative contributions of testosterone and estrogen in regulating bone resorption and formation in normal elderly men. **106,** 1553–1560 (2000).

81. Bord, S., Horner, A., Beavan, S. & Compston, J. Estrogen Receptors Alpha and Beta Are Differentially Expressed in Developing Human Bone. **86,** 2309–2314 (2001).

82. Cowley, S. M., Hoare, S., Mosselman, S. & Parker, M. G. Estrogen Receptors Alpha and Beta Form Heterodimers on DNA. **272,** 19858–19862 (1997).

83. Krum, A. B. K. and S. A. Estrogen Receptors Alpha and Beta in Bone. 130–135 (2017). doi:10.1016/j.bone.2016.03.016.Estrogen

84. Almeida, M. *et al.* Estrogen receptor-alpha signaling in osteoblast progenitors stimulates cortical bone accrual. **123,** (2013).

85. Nicks, K. M. *et al.* Deletion of Estrogen Receptor Beta in Osteoprogenitor Cells Increases Trabecular but Not Cortical Bone Mass in Female Mice. **31,** 606–614 (2016).

86. Martin-millan, M. *et al.* The Estrogen Receptor-Alpha in Osteoclasts Mediates the Protective Effects of Estrogens on Cancellous But Not Cortical Bone. **24,** 323–334 (2015).

87. Wang, Y. *et al.* Opposite Function of Estrogen Receptor Alpha and Estrogen Receptor Beta in Controlling 17 Beta-Estradiol-mediated Osteogenesis in Osteoblasts. **47,** 255–261 (2016).

88. Nakamura, T. *et al.* Estrogen Prevents Bone Loss via Estrogen Receptor Alpha and Induction of Fas Ligand in Osteoclasts. 811–823 (2007). doi:10.1016/j.cell.2007.07.025

89. Harris, H. A., Katzenellenbogen, J. A. & Katzenellenbogen, B. S. Characterization of the Biological Roles of the Estrogen Receptors , Estrogen Receptor alpha and Estrogen Receptor Beta , in Estrogen Target Tissues in Vivo through the Use of an Estrogen Receptor Alpha-Selective Ligand. **143,** 4172–4177 (2002).

90. Sims, N. A. *et al.* A functional androgen receptor is not sufficient to allow estradiol to protect bone after gonadectomy in estradiol receptor – deficient mice. **111,** 1319–1327 (2003).

91. Soltysik K, C. P. Membrane Estrogen Receptors – is it an alternative way of estrogen action ? **1942,** 129–142 (2013).

92. Saczko, J. *et al.* Estrogen Receptors in Cell Membranes : Regulation and Signaling. 93–105 doi:10.1007/978-3-319-56895-9

93. Prossnitz, E. R. & Maggiolini, M. Mechanisms of estrogen signaling via GPR30. **308,** 32–38 (2010).

94. Levin, E. R., L, D. E. E. R., Beach, L. & Beach, L. Estrogen Receptors Associate with and Regulate the Production of Caveolin : Implications for Signaling and Cellular Actions. **16,** 100–115 (2002).

95. Heino, T. J., Chagin, A. S. & Sa, L. The novel estrogen receptor G-protein-coupled receptor 30 is expressed in human bone. 1–6 (2007). doi:10.1677/JOE-07-0629

96. Ford, J. *et al.* GPR30 Deficiency Causes Increased Bone Mass, Mineralization, and Growth Plate Proliferative Activity in Male Mice. **26,** 298–307 (2011).

97. Teplyuk, N. M. *et al.* Runx2 Regulates G Protein-coupled Signaling Pathways to Control Growth of Osteoblast Progenitors. **283,** 27585–27597 (2008).

98. Khan, K., Pal, S., Yadav, M., Maurya, R. & Ku-, A. Prunetin signals via G protein coupled receptor, GPR30: stimulation of adenylyl cyclase and cAMP-mediated activation of MAPK signaling induces Runx2 expression in osteoblasts to promote bone regeneration. *J. Nutr. Biochem.* (2015). doi:10.1016/j.jnutbio.2015.07.021

99. Masuhara, M. *et al.* A relation between osteoclastogenesis inhibition and membrane-type estrogen receptor GPR30. *Biochem. Biophys. Reports* **8,** 389–394 (2016).

100. Pedram, A. *et al.* A Conserved Mechanism for Steroid Receptor Translocation to the Plasma Membrane. (2007). doi:10.1074/jbc.M611877200

101. Kumar, P. *et al.* Direct Interactions with G-Alpha-i and G-Beta Mediate Nongenomic Signaling by Estrogen Receptor Alpha. **21,** 1370–1380 (2007).

102. Gustafsson, K. L., Farman, H., Henning, P., Lionikaite, V. & Wu, J. The role of membrane ER alpha signaling in bone and other major estrogen responsive tissues. 1–11 (2016). doi:10.1038/srep29473

103. Roforth, M. M., Atkinson, E. J., Levin, E. R., Khosla, S. & Monroe, D. G. Dissection of Estrogen Receptor Alpha Signaling Pathways in Osteoblasts Using RNA-Sequencing. **9,** 1–10 (2014).

104. Chan, K. K., Leung, T. H., Chan, D. W. & Wei, N. Targeting estrogen receptor subtypes (ER alpha and ER beta) with selective ER modulators in ovarian cancer. (2014). doi:10.1530/JOE-

13-0500

105. Hernández-fonseca, K., Massieu, L. & De, G. Neuroprotective Role of Estradiol against Neuronal Death Induced by Glucose Deprivation in Cultured Rat Hippocampal Neurons. 41–50 (2012). doi:10.1159/000334229

106. Zhao, F. X. Y., Li, Y. Z., Liu, J. Z. M. & Liu, Y. Nuclear and membrane estrogen receptor antagonists induce reversible changes in synaptic protein expression and actin polymerization in the mouse hippocampus. 495–507 (2018). doi:10.1111/cns.12806

107. Cauley, J. A. Public Health Impact of Osteoporosis. **68,** 1243–1251 (2013).

108. Ji, M. & Yu, Q. Primary osteoporosis in postmenopausal women. **1,** 9–13 (2015).

109. Taciak, B. *et al.* Evaluation of phenotypic and functional stability of RAW 264.7 cell line through serial passages. *PLoS One* **13,** e0198943 (2018).

110. Cao, Z. *et al.* Effects of Resin or Charcoal Treatment on Fetal Bovine Serum and Bovine Calf Serum. **34,** 101–108 (2009).

111. Hayman, A. R. Tartrate-resistant acid phosphatase (TRAP) and the osteoclast / immune cell dichotomy. **41,** 218–223 (2008).

112. Kim, E., Lee, H., Kim, M. H. & Yang, W. M. Inhibition of RANKL-stimulated osteoclast differentiation by Schisandra chinensis through down-regulation of NFATc1 and c-fos expression. 1–8 (2018).

113. Bradford, M. M. Rapid and Sensitive Method for the Quantitation of Microgram Quantities of Protein Utilizing the Principle of Protein-Dye Binding. *Anal. Biochem.* **72,** 248–254 (1976).

114. Gallagher, S. R. Electrophoretic Separation of One-Dimensional SDS Gel Electrophoresis. (2006).

115. Ni, D., Xu, P. & Gallagher, S. Immunoblotting and Immunodetection. in *Current Protocols in Protein Science* **88,** 10.10.1-10.10.37 (John Wiley & Sons, Inc., 2017).

116. Bio-Rad Laboratories. Clarity™ Western ECL Substrate - Instruction Manual. *Bio-Rad* 1–11 (2012).

117. Sarasija, S., Norman, K. R. & Biology, C. C. Measurement of ROS in Caenorhabditis elegans Using a Reduced Form of Fluorescein. **8,** (2018).

118. Wojtala, A. *et al. Methods to Monitor ROS Production by Fluorescence Microscopy and Fluorometry*. *Conceptual background and bioenergetic/mitochondrial aspects of oncometabolism* **542,** (Elsevier Inc., 2014).

119. Vichai, V. & Kirtikara, K. Sulforhodamine B colorimetric assay for cytotoxicity screening. **1,** 1112–1116 (2006).

120. Zhou, Wenchang; Faraldo-Gómez, J. D. Membrane plasticity facilitates recognition of the inhibitor oligomycin by the mitochondrial ATP synthase rotor. 1–21 (2018). doi:10.1016/j.bbabio.2018.03.019.Membrane

121. To, M. *et al.* Mitochondrial uncoupler FCCP activates proton conductance but does not block store-operated Ca 2 + current in liver cells. *Arch. Biochem. Biophys.* **495,** 152–158 (2010).

122. Stanford, K. R. & Taylor-clark, T. E. Mitochondrial modulation-induced activation of vagal sensory neuronal subsets by antimycin A , but not CCCP or rotenone , correlates with mitochondrial superoxide production. 1–18 (2018).

123. Camassa, J. A. *et al.* Tartrate-resistant acid phosphate as biomarker of bone turnover over the lifespan and different physiologic stages in sheep. *BMC Vet. Res.* 1–8 (2017). doi:10.1186/s12917-017-1170-9

124. Panwar, P. *et al.* An Ectosteric Inhibitor of Cathepsin K Inhibits Bone. *J. Bone Miner. Res.* (2017). doi:10.1002/jbmr.3227

125. Lemma, S. *et al.* Energy metabolism in osteoclast formation and activity. *Int. J. Biochem. Cell Biol.* **79,** 168–180 (2016).

126. Jin, Z., Wei, W., Yang, M., Du, Y. & Wan, Y. Mitochondrial Complex I Activity Suppresses Inflammation and Enhances Bone Resorption by Shifting Macrophage-Osteoclast Polarization. *Cell Metab.* **20,** 483–498 (2014).

127. Rooney, JP; Ryde, IT; Sanders, LH; Howlett, EH; Colton,MD; Germ, KE; Mayer, GD; Greenamyre, JT; and Meyer, J. PCR Based Determination of Mitochondrial DNA Copy Number in Multiple Species. *Methods Mol Biol* 1–14 (2015). doi:10.1007/978-1-4939-1875-1

128. Kong, L. *et al.* Picrasidine I from Picrasma Quassioides Suppresses Osteoclastogenesis via Inhibition of RANKL Induced Signaling Pathways and Attenuation of ROS Production. *Cell. Physiol. Biochem.* 1425–1435 (2017). doi:10.1159/000481874

129. Unfer, T. C. *et al.* Estrogen plus progestin increase superoxide dismutase and total antioxidant capacity in postmenopausal women. *Int. Menopause Soc.* 1–10 (2014). doi:10.3109/13697137.2014.964669

130. Collin-osdoby, P. & Osdoby, P. RANKL-Mediated Osteoclast Formation from Murine RAW 264.7 cells. *Bone Res. Protoc.* **816,** 187–202 (2011).

131. Vincent, C., Kogawa, Æ. M., Findlay, D. M. & Atkins, Æ. G. J. The generation of osteoclasts from RAW 264 . 7 precursors in defined , serum-free conditions. *J Bone Min. Metab* 114–119 (2009). doi:10.1007/s00774-008-0018-6

132. Junrui, P. *et al.* Relationship between fluoride exposure and osteoclast markers during RANKL-induced osteoclast differentiation. *Environ. Toxicol. Pharmacol.* **46,** 241–245 (2016).

133. Rahman, M. M. *et al.* Proliferation-coupled osteoclast differentiation by RANKL : Cell density as a determinant of osteoclast formation. *Bone* **81,** 392–399 (2015).

134. Tanaka, S. *et al.* Molecular Mechanism of the Life and Death of the Osteoclast. *New York Acad. Sci.* **186,** 180–186 (2006).

135. Folmes CD, Dzeja PP, Nelson TJ, T. A. Metabolic Plasticity in Stem Cell Homeostasis and Differentiation. **11,** 596–606 (2013).

136. Ahn, H., Lee, K., Kim, J. M., Kwon, S. H. & Lee, S. H. Accelerated Lactate Dehydrogenase Activity Potentiates Osteoclastogenesis via NFATc1 Signaling. *PLoS One* 1–13 (2016). doi:10.1371/journal.pone.0153886

137. Indo, Y. *et al.* Metabolic Regulation of Osteoclast Differentiation and Function. *J. Bone Miner. Res.* (2013). doi:10.1002/jbmr.1976

138. Czupalla, C., Mansukoski, H., Pursche, T., Krause, E. & Hoflack, B. Comparative study of protein and mRNA expression during osteoclastogenesis. *Proteomics* 3868–3875 (2005). doi:10.1002/pmic.200402059

139. Andrew YH Ng, Chengjian Tu, Shichen Shen, Ding Xu, Merry J Oursler, J. Q. & Yang, and S. Comparative Characterization of Osteoclasts Derived From Murine Bone Marrow Macrophages and RAW 264.7 Cells Using Quantitative Proteomics. **2,** 328–340 (2018).

140. Srinivasan, Satish; Guha, Manti; Kashina, Anna; Avadhani, N. G. Mitochondrial Dysfunction

and Mitochondrial Dynamics-The Cancer Connection. **1858,** 602–614 (2018).

141. Wallace, D. C. & Fan, W. ENERGETICS, EPIGENETICS, MITOCHONDRIAL GENETICS. **10,** 12–31 (2011).

142. Zeng, R., Faccio, R. & Novack, D. V. Alternative NF-κB Regulates RANKL-induced Osteoclast Differentiation and Mitochondrial Biogenesis via Independent Mechanisms. *J Bone Min. Res* **30,** 2287–2299 (2016).

143. Brown, D. & Breton, S. REVIEW MITOCHONDRIA-RICH , PROTON-SECRETING EPITHELIAL CELLS. *J. Exp. Biol.* **2358,** 2345–2358 (1996).

144. Kim, M. S. *et al.* RANKL-mediated Reactive Oxygen Species Pathway That Induces Long Lasting Ca 2+ Oscillations Essential for Osteoclastogenesis. *J. Biol. Chem.* **285,** 6913–6921 (2010).

145. Sasaki, H. *et al.* NADPH oxidase-derived reactive oxygen species are es- sential for differentiation of a mouse macrophage cell line (RAW264 . 7) into osteoclasts. *J. Med. Investig.* **56,** 33–41 (2009).

146. Przedborski, S., & Schon, E. A. Loss of ROS- a radical respose. *Nature* (1998).

147. Sharma, R. *et al.* Caspase-2 Maintains Bone Homeostasis by Inducing Apoptosis of Oxidatively-Damaged Osteoclasts. *PLoS One* **9,** 1–11 (2014).

148. Champy, R., Mitrovic, D., Collin, P. & Lomri, A. Reactive oxygen species and superoxide dismutases : Role in joint diseases. **74,** 324–329 (2007).

149. Almeida, M., Han, L., Ambrogini, E., Bartell, S. M. & Manolagas, S. C. Oxidative Stress Stimulates Apoptosis and Activates NF-kB in Osteoblastic Cells via a PKCb/p66shc Signaling Cascade: Counter Regulation by Estrogens or Androgens. **24,** 2030–2037 (2015).

150. Lee, S. R. *et al.* Dietary intake of genistein suppresses hepatocellular carcinoma through AMPK- mediated apoptosis and anti-inflammation. 1–12 (2019).

151. Li, J. *et al.* Genistein suppresses tumor necrosis factor α -induced inflammation via modulating reactive oxygen species / Akt / nuclear factor κ B and adenosine monophosphate-activated protein kinase signal pathways in human synoviocyte MH7A cells. 315–323 (2014).

152. Almeida, M. *et al.* Estrogens and androgens in skeletal physiology and pathophysiology. 135–187 (2017). doi:10.1152/physrev.00033.2015

153. Imbert-fernandez, Y. *et al.* Estradiol Stimulates Glucose Metabolism via 6-Phosphofructo-2-kinase (PFKFB3). **289,** 9440–9448 (2014).